

See discussions, stats, and author profiles for this publication at: <https://www.researchgate.net/publication/261028315>

A Solubility Comparison of Neutral and Zwitterionic Polymorphs

ARTICLE *in* CRYSTAL GROWTH & DESIGN · MARCH 2014

Impact Factor: 4.89 · DOI: 10.1021/cg5000205

CITATIONS

9

READS

200

1 AUTHOR:



Dr Sudalai Kumar S

The Francis Xavier Engineering College

32 PUBLICATIONS **57 CITATIONS**

SEE PROFILE

A Solubility Comparison of Neutral and Zwitterionic Polymorphs

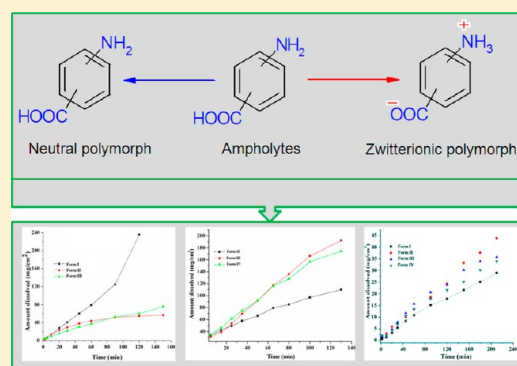
Published as part of the Crystal Growth & Design virtual special issue IYCr 2014 - Celebrating the International Year of Crystallography.

S. Sudalai Kumar and Ashwini Nangia*

School of Chemistry, University of Hyderabad, Central University PO, Prof. C. R. Rao Road, Gachibowli, Hyderabad 500 046, India

Supporting Information

ABSTRACT: Several amphoteric model compounds and drugs, such as isomers of aminobenzoic acids (ortho, meta, and para), *N*-aryl-2-amino-nicotinic acids (three isomers), amino-salicylic acids (meta and para), clonixin, and niflumic acid, were selected to obtain their zwitterionic and neutral polymorphs with the objective to study their X-ray crystal structures, solubility and dissolution rate, and stability. We were successful in crystallizing neutral and ionic polymorphs for 2- and 3-aminobenzoic acid (ABA), 2-(*p*-tolylamino)nicotinic acid (TNA), and clonixin (CLX), as well as 4- and 5-aminosalicylic acid (4-ASA as neutral and 5-ASA in ionic form). The neutral and zwitterionic crystalline polymorphs were differentiated by their distinctive powder X-ray diffraction (PXRD), Fourier transform infrared, Raman and ss-NMR spectroscopy, and further quantified by Hirshfeld surface analysis. Phase transitions were monitored by differential scanning calorimetry and variable temperature powder X-ray diffraction. The difference in solubility and dissolution rates of the neutral and zwitterionic polymorphs were correlated with their hydrogen bonding ($\text{O}-\text{H}\cdots\text{O}$, $\text{O}-\text{H}\cdots\text{N}$, and $\text{N}^+-\text{H}\cdots\text{O}^-$). The faster dissolution rates of the ionic forms were ascribed to stronger, attractive interactions between the solvent molecules and the zwitterionic functional groups. Even as there is no general strategy yet to crystallize ionic polymorphs of amphoteric molecules, the present study shows the advantages of zwitterionic forms for solubility enhancement.



INTRODUCTION

Polymorphism is a solid-state phenomenon exhibited by over half the pharmaceuticals. Polymorphs differ in their X-ray crystal structures, physicochemical properties such as stability, solubility, dissolution, and bioavailability, as well as filterability, compaction, tableting, etc.¹ The differences in these properties arise due to the differences in crystal packing, molecular conformation, morphology, and stability of polymorphs.² For example, the conformational difference in the polymorphs of Ritonavir and Nimesulide causes differences in their solubility and dissolution rates.^{3a,b} Differences in crystal packing can induce different solubility and dissolution rates of polymorphs.^{3c-e} The solubility and dissolution rates of drug forms are related inversely with their stability; that is, metastable polymorphs are more soluble, whereas the thermodynamic form is the least soluble.⁴ The higher solubility of metastable polymorphs is due to their higher thermodynamic functions and free energy.^{2,3} In the case of ampholytes, that is, molecules with both acidic and basic groups in the same structure, they can exist in neutral, zwitterionic, or dual states. Amino acids are the simplest examples of ampholytes, but they exist in the zwitterionic form only in the crystal structure.⁵ We initiated a study of amphoteric model compounds and drugs to study neutral and zwitterionic solid-state forms, proton state of acidic/basic groups in these structures, and the solubility and dissolution

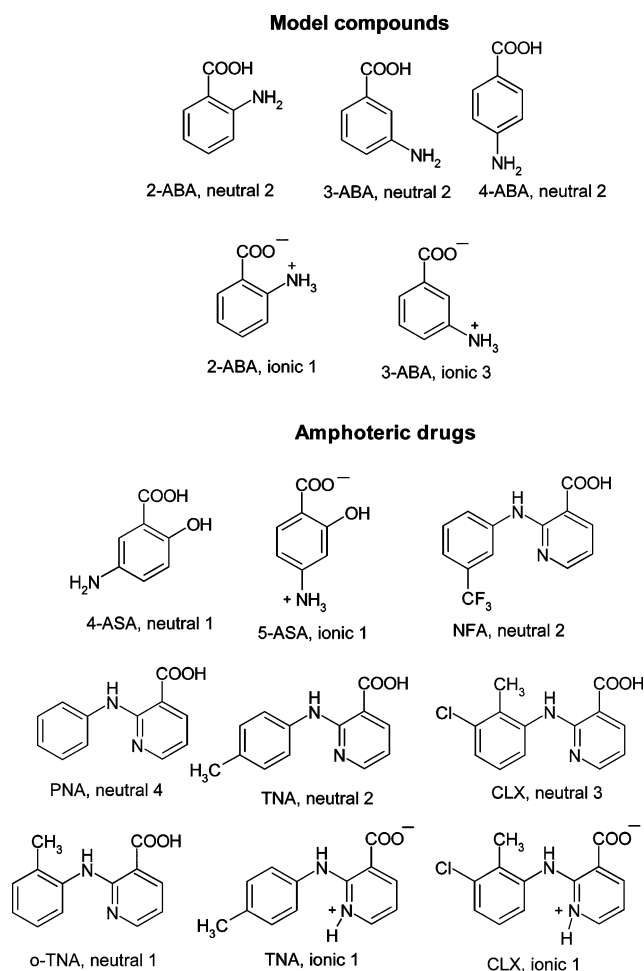
rate of such neutral/zwitterions polymorph pairs.^{6,7} Over 40 drug molecules are amphoteric (see Table S1, Supporting Information) with high/moderate solubility and low permeability, and thus selection of the optimal crystalline form for solubility optimization⁸ is an end goal in such studies. A disadvantage with zwitterionic drug forms could be that their low permeability will affect druggability and bioavailability.⁹ However, because of facile proton transfer as a function of pH, some zwitterionic drugs are more permeable than their neutral structures.¹⁰

On the basis of the above idea and the importance of amino acids and diarylamines in medicine and solid-state chemistry, a few amphoteric molecules (Scheme 1) were selected and screened by several crystallization techniques to obtain neutral and/or zwitterionic crystal structures.^{7,11,12} The drugs include clonixin (CLX, anti-inflammatory), 4-aminosalicylic acid (4-ASA, antituberculosis), mesalazine (5-ASA, anti-inflammatory), along with 2-aminobenzoic acid (2-ABA) and 3-aminobenzoic acid (3-ABA) as model compounds, whose crystal structures were recently reported.^{6,7,12} The known polymorphs for these ampholytes are three neutral forms and one zwitterionic form

Received: January 6, 2014

Revised: March 7, 2014

Scheme 1. Polymorphic Neutral and Zwitterionic Crystal Structures Discussed in This Study^a



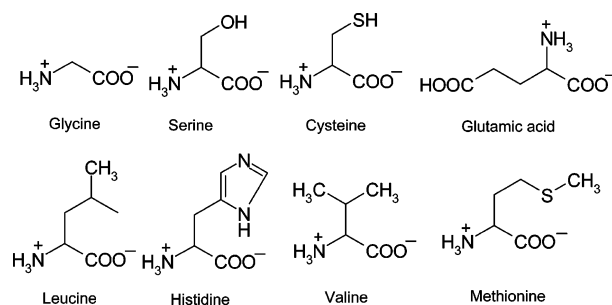
^a4-ASA and 5-ASA are monomorphic but isomeric structures. The X-ray crystal structures are reported in refs 6a,b,e, 7,a,d,e, and 12a,e. The number of reported polymorphs is mentioned in parentheses below the compound for each type.

of CLX, two neutral forms and one zwitterionic form for TNA, a neutral form for 4-ASA, a zwitterionic structure of 5-ASA, one zwitterionic-neutral and two neutral forms of 2-ABA, and three zwitterionic forms plus two neutral forms of 3-ABA (Scheme 1). We were successful in reproducing three of the reported cases to obtain one zwitterionic and another neutral polymorph for the same molecule (2-ABA, 3-ABA, TNA, and CLX). These sets of neutral and zwitterionic polymorphs were characterized by Fourier transform infrared (FT-IR), Raman, solid-state ¹³C NMR, and powder X-ray diffraction (PXRD). Thermal phase transitions between the neutral and zwitterionic polymorphs were studied by variable temperature powder X-ray diffraction (VT-PXRD) and differential scanning calorimetry (DSC).¹³ Attempts to crystallize a novel polymorph of 4-ASA and 5-ASA were not successful (both are single crystal structure drugs), so these isomeric drugs were used as such to compare solubility trends between neutral and zwitterionic isomeric compounds. The solubility and dissolution rates of neutral and zwitterionic polymorphs are correlated with crystal packing, hydrogen bonding, and molecular conformation in the crystal structure.

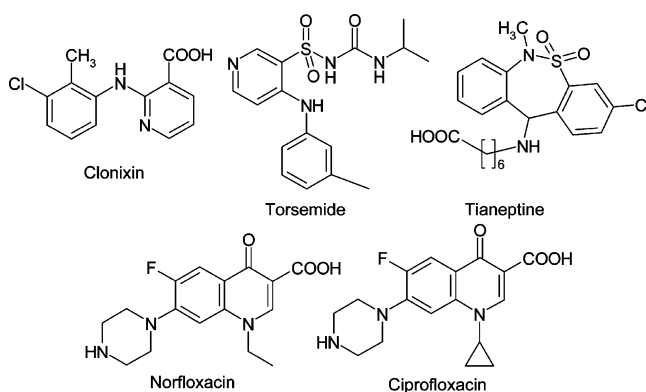
RESULTS AND DISCUSSION

Neutral and Zwitterionic Polymorphs. Polymorphism in amino acids is common, but the existence of both neutral and

Scheme 2. Zwitterionic Polymorphs of Eight Amino Acids in the CSD (May 2013 Update)



Scheme 3. Neutral and Zwitterionic Polymorphs of Five Drugs in the CSD (May 2013 Update)



zwitterionic forms has so far not been observed in the crystal structures of these biomolecules. Glycine, leucine, serine, histidine, cysteine, and glutamic acid are enantiomerically pure crystalline zwitterionic polymorphs (Scheme 2), and valine, serine, cysteine, and methionine are racemic crystalline polymorphs known among the 20 proteinogenic amino acids. Among the amphoteric drugs, a few examples were extracted as neutral and zwitterionic crystal structure sets from the Cambridge Structural Database (CSD ver. 5.34, May 2013 update). Notably clonixin, ciprofloxacin, norfloxacin, torsemide, and tianeptine (Scheme 3) are examples of neutral and zwitterionic drug polymorphs.⁶ Moreover, three of the model organic compounds studied in recent papers,^{6,7} namely, 2-ABA, 3-ABA, and 2-(*p*-tolylamino)nicotinic acid fall in the category of zwitterionic/neutral polymorph pairs (Scheme 1). The intramolecular proton transfer in these molecular crystals suggested the possibility to control solubility and stability based on proton-transfer mediated polymorphism.⁶ Given the small number of marketed drugs in this category, we expanded the case studies to model compounds as well. 2-(*p*-Tolylamino)-nicotinic acid was reported recently by us^{6a} and anthranilic acids by Harris et al.^{6b} A recent study suggests that crystallization of the zwitterionic polymorph of Tianeptine was controlled by pH.^{6c} We crystallized ampholyte compounds under different crystallization conditions to obtain neutral and ionic polymorphs for studying their physicochemical properties. We were unable to develop a general protocol for the controlled crystallization of neutral or ionic polymorph.

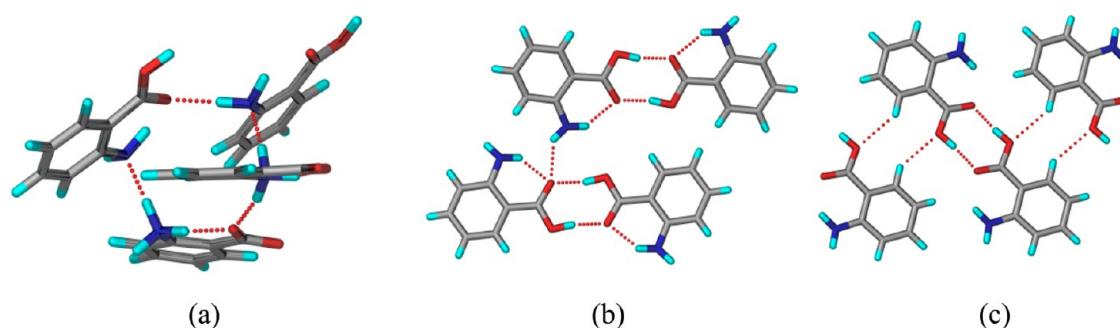


Figure 1. 2-Aminobenzoic acid polymorphs. Neutral ($\text{N}-\text{H}\cdots\text{O}$) and ionic ($\text{N}^+-\text{H}\cdots\text{O}^-$ and $\text{N}^+-\text{H}\cdots\text{N}$) hydrogen bonds in Form I having $\text{R}_6^4(12)$ motif (a), and $\text{O}-\text{H}\cdots\text{O}$ carboxylic acid dimer synthon of $\text{R}_2^2(8)$ notation in Form II (b) and Form III (c).

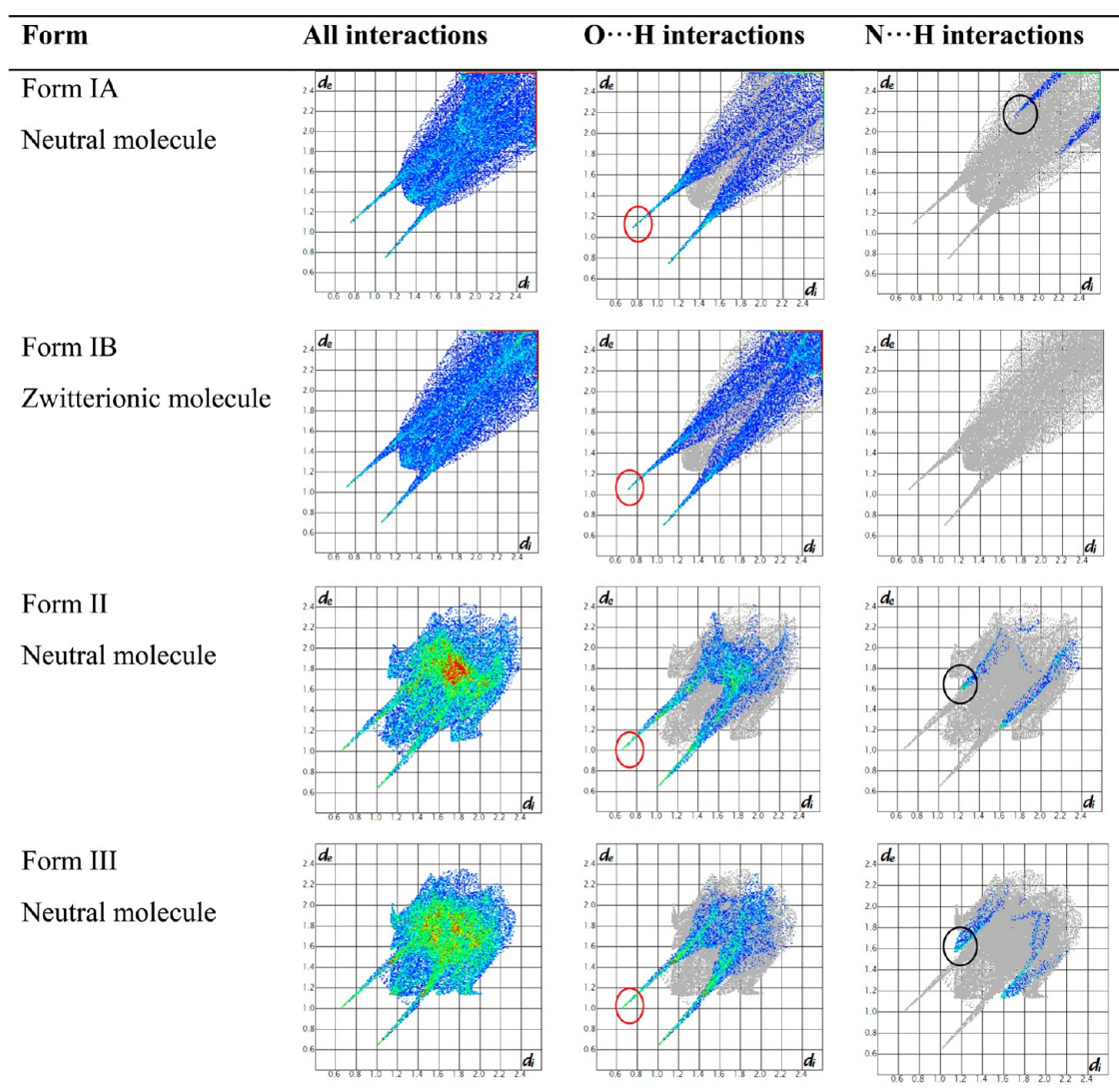


Figure 2. Hirshfeld 2D fingerprint plot for differentiating neutral $\text{N}-\text{H}\cdots\text{O}$ interactions from the ionic $\text{N}^+-\text{H}\cdots\text{O}^-$ and $\text{N}^+-\text{H}\cdots\text{N}$ interactions for 2-ABA trimorphs.

Crystallization and Structural Analysis of Ampholytes. 2-Aminobenzoic Acid (2-ABA) Polymorphs. The trimorphs of 2-ABA were reproduced by solvent crystallization and melting/heating techniques.^{7a} Form I was crystallized from methanol or ethanol. Form II was produced in polar solvents such as EtOAc, i-PrOH, and nitromethane. Form III was obtained by melt crystallization at 135 °C for 30 min. The bulk purity of all three polymorphs was checked by PXRD and DSC. The crystalline

forms of 2-ABA have been reported by different groups.⁷ Hardy et al.^{7a} studied luminescent behavior of three polymorphs collectively and identified the ionic Form I as triboluminescent, whereas the two neutral forms were non-triboluminescent based on their polarity. Ojala and Etter^{7b} reexamined all three polymorphs in terms of phase transition and reported the single-crystal to single-crystal transformation of Form II to I. Carter and Ward^{7c} demonstrated the importance of surface

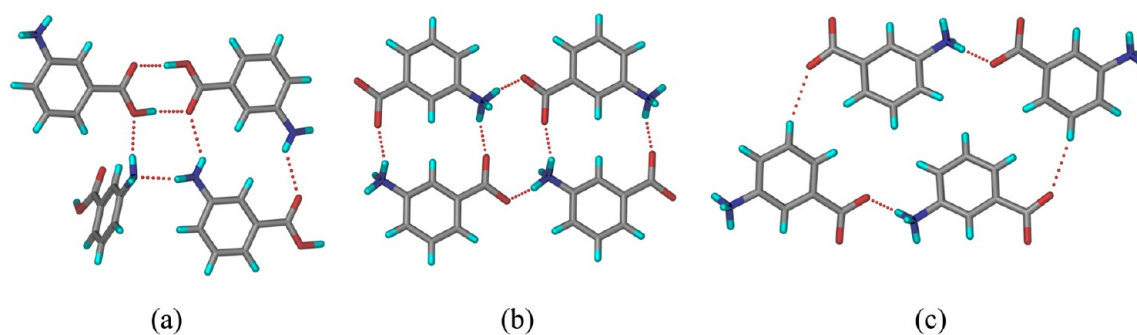


Figure 3. 3-Aminobenzoic acid polymorphs. Acid dimer O–H...O synthon $R_2^2(8)$ motif, neutral N–H...O bonds in Form II (a) and ionic $N^+–H...O^-$ in Form III (b) and Form IV (c).

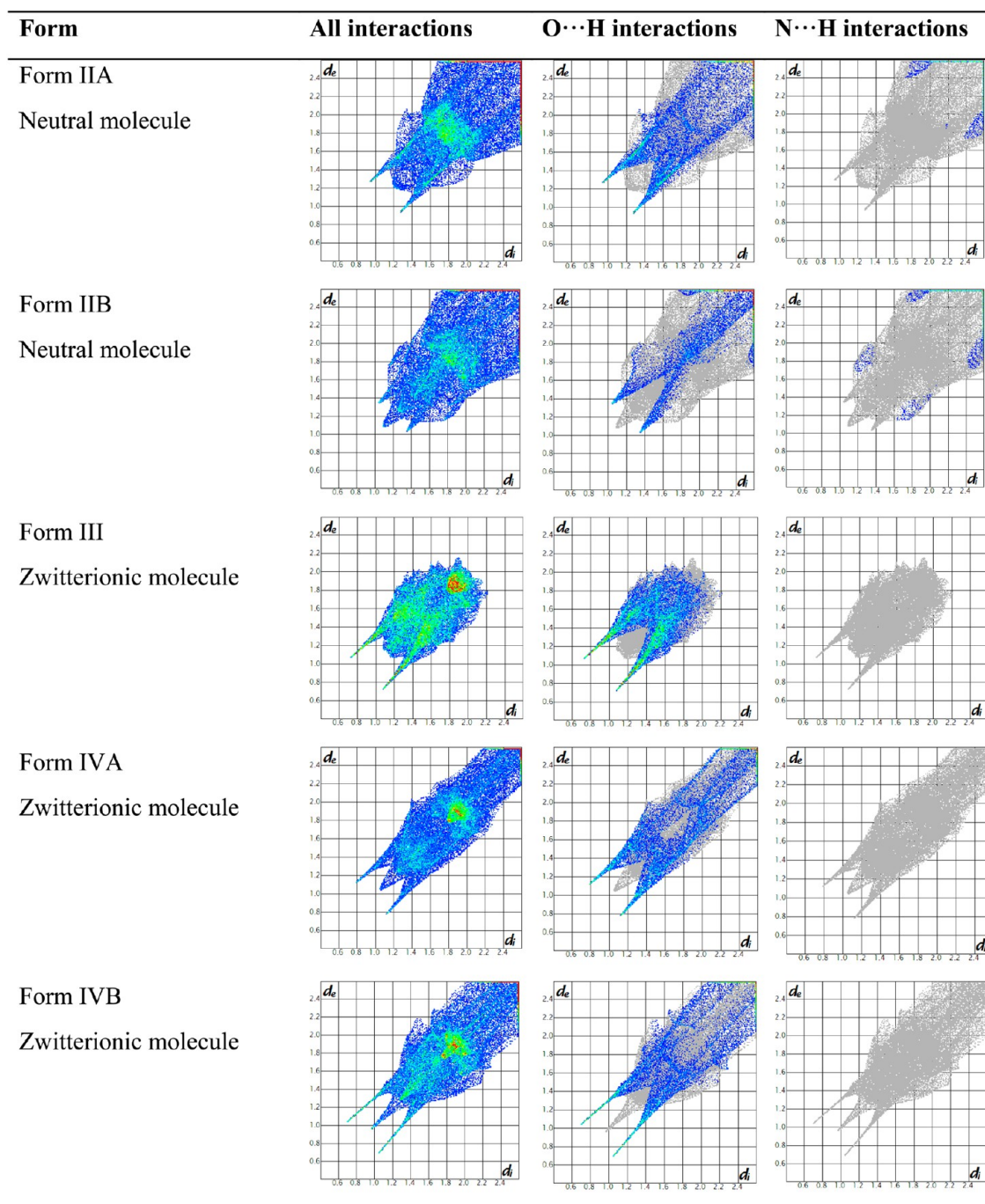


Figure 4. Hirshfeld 2D fingerprint plot for differentiating the O–H...O and $N^+–H...O^-$ H bonds in neutral and ionic structure of 3-ABA trimorphs.

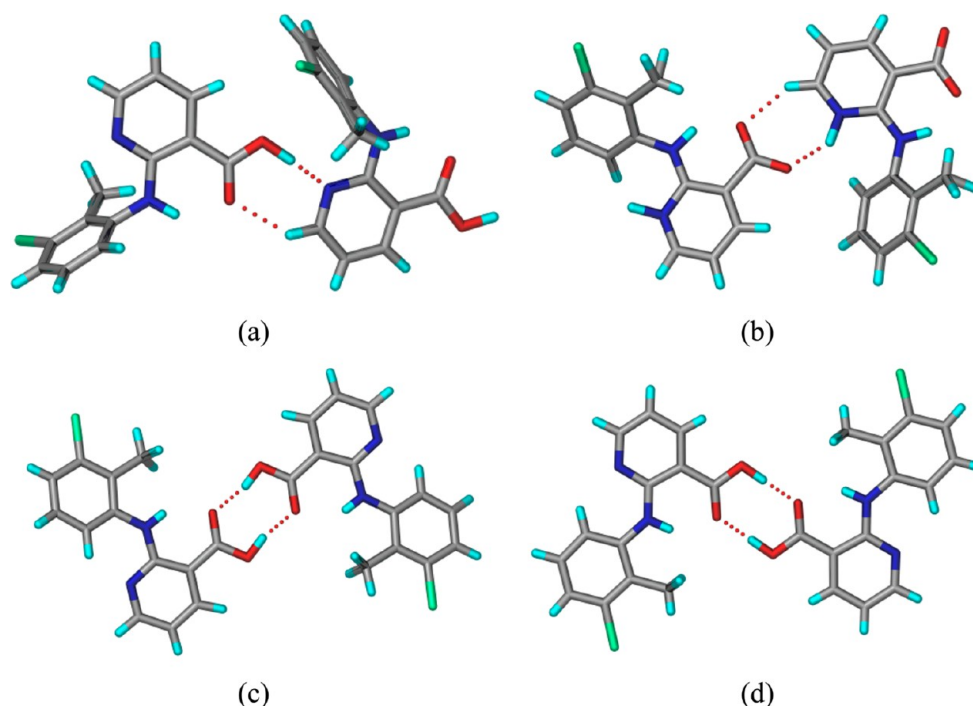


Figure 5. Clonixin polymorphs. Strong acid–pyridine O–H...N synthon in Form I (a), acid–pyridine ionic N⁺–H...O[−] H bond in Form II (b), and acid dimer O–H...O R₂²(8) motif in Form III (c) and Form IV (d).

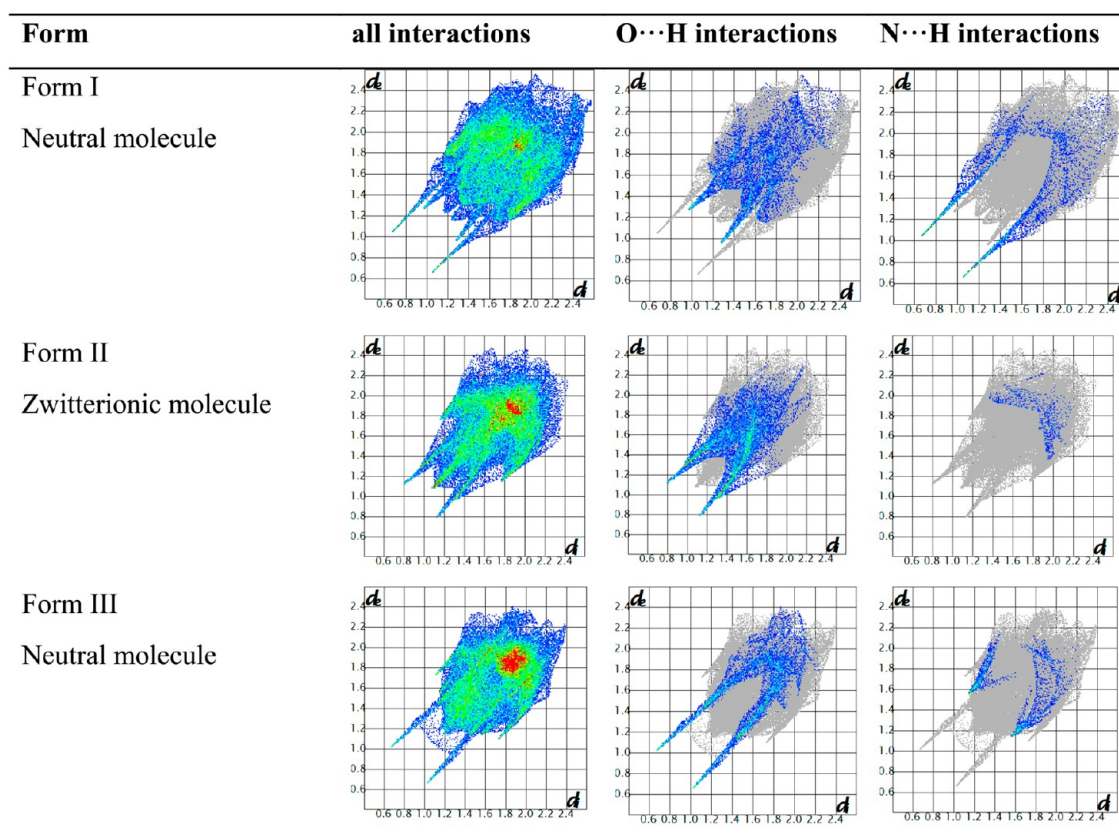


Figure 6. Hirshfeld 2D fingerprint plots for differentiating the neutral acid–pyridine O–H...N hydrogen bond from the ionic N⁺–H...O[−] and O–H...O in clonixin polymorphs. Form IV is not included because H atoms could not be located in the crystal structure.

functionality on polymorph selectivity and growth orientation in anthranilic acid polymorphs. Neutral O–H...N and ionic N⁺–H...O[−] hydrogen bonds stabilize the solid-state structures

(Figure 1; the cif files were extracted from the CSD; Refcodes AMBACO01, AMBACO05, and AMBACO08).¹⁴ Form I (*Z'* = 2) and II (*Z'* = 1) are reported as orthorhombic structures in *P2₁cn*

Table 1. Crystallographic Parameters Reported in the CSD for Clonixin Polymorphs

2-(2-methyl-3-chloroanilino)-nicotinic acid	Form I	Form II	Form III	Form IV
CSD Refcode ¹⁴	BIXGIY	BIXGIY04	BIXGIY02	BIXGIY03
formula weight	C ₁₃ H ₁₁ ClN ₂ O ₂	C ₁₃ H ₁₁ ClN ₂ O ₂	C ₁₃ H ₁₁ ClN ₂ O ₂	C ₁₃ H ₁₁ ClN ₂ O ₂
crystal system	monoclinic	orthorhombic	triclinic	triclinic
space group	<i>P</i> 2 ₁ / <i>c</i>	<i>Pca</i> 2 ₁	<i>P</i> $\bar{1}$	<i>P</i> $\bar{1}$
<i>a</i> (Å)	7.625(1)	23.597(6)	13.810(1)	7.670(1)
<i>b</i> (Å)	14.201(1)	4.042(1)	3.858(1)	7.254(1)
<i>c</i> (Å)	11.672(1)	12.127(3)	10.984(2)	10.882(1)
α (°)	90	90	94.98(1)	100.66(1)
β (°)	101.65(1)	90	94.42(1)	102.02(1)
γ (°)	90	90	95.57(1)	86.97(1)
<i>V</i> (Å ³)	1237.8	1156.6	578.1	581.8
<i>D</i> _{calcd} (g cm ⁻³)	1.41	1.51	1.51	1.50
<i>Z</i> / <i>Z'</i>	4/1	4/1	2/1	2/1
<i>wR</i> ₂ (all)	5.2	6.5	7	4.8
<i>T</i> (K)	298	298	298	298

and *Pbca* space groups ($a = 12.868$, $b = 10.772$, $c = 9.325$ Å; and $a = 15.992$, $b = 11.624$, $c = 7.160$ Å), whereas the third form ($Z' = 1$) is in *P*2₁/*c* space group ($a = 6.537$, $b = 15.351$, $c = 7.086$ Å; $\beta = 112.64^\circ$). Form I has one neutral and one zwitterionic molecule in the asymmetric unit. Form I contains neutral (N–H \cdots O) and ionic (N⁺–H \cdots O[−] and N⁺–H \cdots N) H bonds in the R₆⁴(12) ring motif, whereas Forms II and Form III contain the centrosymmetric carboxylic acid O–H \cdots O dimer synthon of R₂²(8) notation in the crystal structure¹⁵ (Figure 1).

The contribution of intermolecular interactions was quantified by Hirshfeld surface analysis¹⁶ and 2D fingerprint plots to differentiate the two distinct asymmetric unit molecules (A and B) of Form I compared to those in Form II and III (Figure 2). The sharp spikes in the 2D fingerprint plot of Forms I, II, and III at $d_e = d_i \approx 1.0$ Å indicates short N–H \cdots O/N⁺–H \cdots O[−] interactions (highlighted by red circles). The sharp spikes for Form IA, II, and III at $d_e = d_i \approx 1.6$ and 2.2 Å indicate the presence of N⁺–H \cdots N interactions in the neutral structures of Forms IA, II, and III (highlighted by black circles). The absence of sharp spikes for N–H \cdots N interactions in Form IB is a clear indication of protonated amine, which does not accept hydrogen bonds.

3-Aminobenzoic Acid (3-ABA) Polymorphs. The three polymorphs were reproduced by crystallization through solvent evaporation and melting. We are unable to reproduce polymorphs I and V by the reported method of solvent evaporation from methanol and melting of Form III, respectively.^{6b} Form II was produced by melt crystallization at 170 °C for 30 min, and Form III was crystallized in acetonitrile solvent while Form IV was crystallized using EtOAc solvent in our hands. The bulk purity of the polymorphs was checked by PXRD and DSC. Harris et al.^{6b} reported recently the crystal structures of three new polymorphs, Form III (AMBNZA01), Form IV (AMBNZA02), and Form V (AMBNZA03), determined by PXRD data structure solution. They compared the crystal structures and thermal stability of these new polymorphs with the reported polymorph I (no crystal structure in CSD) and II (AMBNZA). Form II ($Z' = 2$, *P*2₁/*c*, $a = 5.047$, $b = 23.06$, $c = 11.790$ Å, $\beta = 105.47^\circ$) and V ($Z' = 1$, *P*2₁/*a*, $a = 14.787$, $b = 4.956$, $c = 9.081$ Å, $\beta = 95.21^\circ$), respectively. Forms III ($Z' = 1$, *P*2₁/*a*, $a = 21.339$, $b = 7.296$, $c = 3.777$, $\beta = 94.82^\circ$) and IV ($Z' = 2$, *P* $\bar{1}$, $a = 3.800$, $b = 11.55$, $c = 14.633$ Å, $\alpha = 110.50^\circ$, $\beta = 92.74^\circ$, $\gamma = 96.59^\circ$) were crystallized as zwitterionic forms. Two molecules in the asymmetric unit of neutral Form II interact

Table 2. Torsion Angles for Molecular Conformations of Clonixin Tetramorphs

clonixin polymorph	torsion angle C2–N2–C6–C7 (deg)
Form I	71.27
Form II	140.26
Form III	160.24
Form IV	178.81

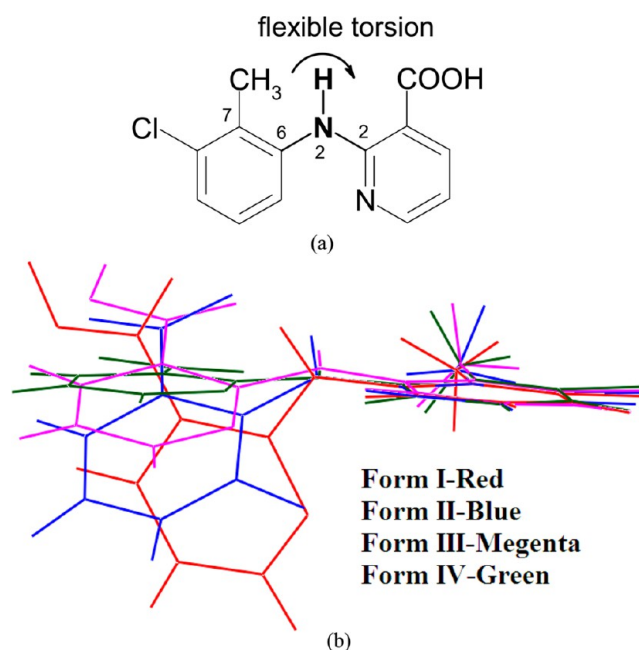


Figure 7. (a) Torsional flexibility in clonixin tetramorphs, and (b) the overlay of different molecular conformations in CLX tetramorphs.

through the O–H \cdots O acid dimer of a R₂²(8) ring motif (Figure 3). The zwitterionic molecules in Form III contains ionic N⁺–H \cdots O[−] H bonds in a R₄⁴(8) ring motif. Two independent molecules of zwitterionic Form IV form a linear C(7) chain through ionic N⁺–H \cdots O[−] interactions. The crystal structure of Form I is not disclosed so far, and the crystal structure of Form V is excluded from this discussion due to disorder. The wings expected at $d_e = d_i \approx 1.6$ and 2.4 Å for N–H \cdots N interactions are absent in the Hirshfeld 2D fingerprint plots (Figure 4) for 3-ABA

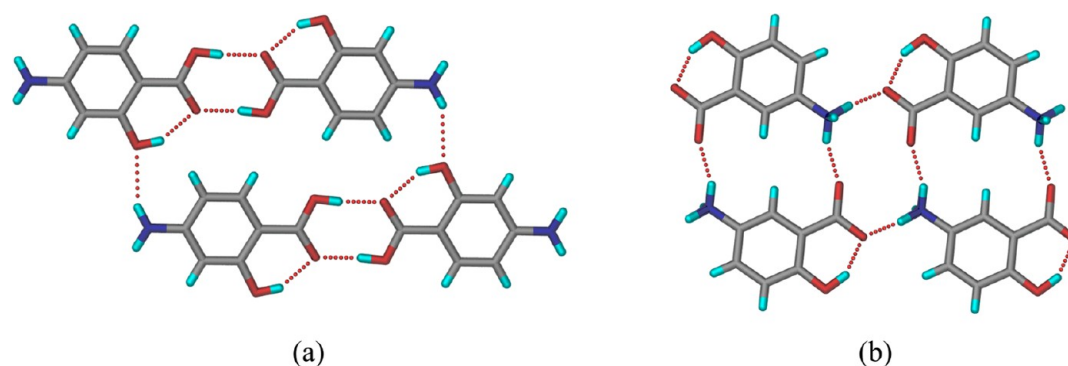


Figure 8. Carboxylic acid dimer O–H...O synthon of $R_2^2(8)$ ring motif and neutral N–H...O interactions in 4-ASA (a) are replaced by ionic $N^+–H...O^-$ interactions in $R_4^4(12)$ ring motif for 5-ASA (b).

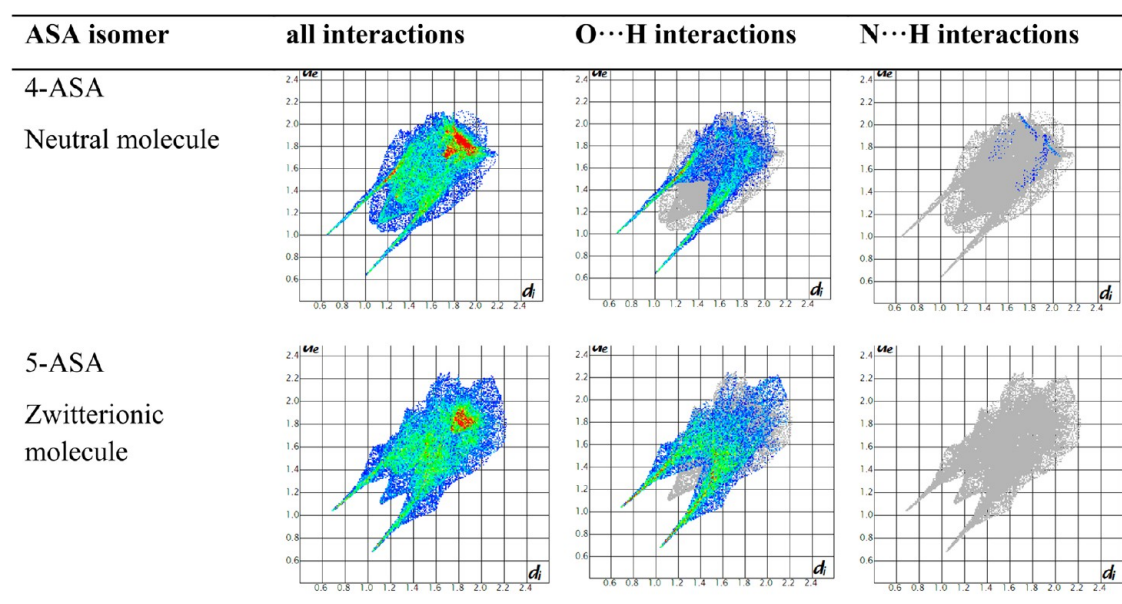


Figure 9. Hirshfeld surface 2D fingerprint plots show un-ionized N...H interactions in 4-ASA (top) the absence of ionized N...H interactions in 5-ASA (bottom).

zwitterionic polymorphs, which means the absence of zwitterionic interactions in Forms III and IV due to a protonated amine/iminium ion.

Clonixin (CLX) Polymorphs. Clonixin polymorphs^{6e} are reported in the literature. We recently synthesized this compound and crystallized it from different organic solvents.^{6a} The reproducibility of crystallization on a bulk scale for solubility measurements posed challenges under the reported conditions of single crystal growth. After some experimentation, we crystallized Form I from acetone, EtOAc, and nitromethane, and Form II from acetic acid; the other two neutral forms were produced in toluene and MeOAc, respectively. The purity and stability of these polymorphs were monitored by PXRD and DSC. Form I neutral structure contains strong acid–pyridine synthon (O–H...N), whereas Form II ionic structure contains an acid–pyridine ionic $N^+–H...O^-$ H bond in the crystal structure (Figure 5). The Hirshfeld 2D fingerplots for Forms I and II are different for these neutral and ionic polymorphs (Figure 6). The sharp spike at $d_e = d_i \approx 1.0$ Å is for N...H contribution in Form I, but this spike is absent in the Form II fingerprint plot. The third and fourth neutral forms of clonixin have the centrosymmetric O–H...O carboxylic acid dimer

synthon. The reported unit cell values of these tetramorphs are listed in Table 1.

Molecular Conformations of Clonixin. The molecular conformation is different in neutral and zwitterionic polymorphs of clonixin at the flexible C2–N2–C6–C7 bonds. This fluxional change in the clonixin molecule results in conformational polymorphs¹⁷ (see Table 2 for torsion angles and overlay diagram in Figure 7) along with the synthon changing from carboxylic acid dimer to acid–pyridine in four polymorphs. The influence of molecular conformation on drug solubility and dissolution rate was discussed in a recent paper: in general, twisted conformation gave a more soluble crystalline form compared to the planar state.¹⁸ The twisted and planar conformations of clonixin polymorphs could tune drug solubility.

Aminosalicilic Acid Isomers. 4-ASA was crystallized in several organic solvents to obtain a new zwitterionic polymorph under ambient and freeze evaporation conditions. However, only the known neutral form was crystallized in all experiments.¹² 5-ASA has limited solubility in organic solvents. It is freely soluble in water and tends to degrade under ambient conditions. The color change of the solution indicated degradation to 3-aminophenol upon heating/boiling the

Table 3. ΔpK_a of a Few Amphoteric Molecules and Drugs^{a,b} and Proton Transfer in the Crystal Structure

s. no.	amphoteric compound	neutral crystal structure	zwitterionic crystal structure	calculated pK_a of acid and conjugate acid of the base	ΔpK_a
1	2-aminobenzoic acid (2-ABA)	Forms II and III	Form I	4.89 (COOH) 1.95 (NH ₂)	−2.94
2	3-aminobenzoic acid (3-ABA)	Forms II and V	Form I, III, and IV	4.81 (COOH) 3.27 (NH ₂)	−2.86
3	2-(<i>p</i> -tolylamino) nicotinic acid (TNA)	Forms I and II	Form III	1.89 (COOH) 5.52 (Py N)	3.63
4	clonixin (CLX)	Forms I, III, and IV	Form II	1.88 (COOH) 5.51 (Py N)	3.63
5	tianeptine	Form A	Form B	4.22 (COOH) 8.10 (NH)	3.88
6	torsemide	Form II	Form I and III	5.92 (−CONHCO−) 4.20 (Py N)	−1.72
7	norfloxacin	Forms B and C	Form A	5.77 (COOH) 8.68 (Pip NH)	2.91
8	ciprofloxacin	Form II	Form I	5.76 (COOH) 8.68 (Pip NH)	2.92
9	4-aminosalicylic acid (4-ASA)	Form I	not known	2.02 (COOH) 5.87 (NH ₂)	3.85
10	5-aminosalicylic acid (5-ASA)	not known	Form I	3.68 (COOH) 2.19 (NH ₂)	−1.49

^a pK_a values are calculated using ChemAxon (Marvin 6.0.1, 2013, ChemAxon software <http://www.chemaxon.com>). ^bFor reference, the experimental pK_a of pyridine in water is 5.22 (calc. 5.12) and that of aniline is 4.58 (calc. 4.64).

solution to dissolve more of the compound for crystallization.¹² The carboxylic acid dimer O—H...O synthon of the $R_2^2(8)$ ring motif with N—H...O interaction in the 4-ASA structure is different from the ionic $N^+—H...O^-$ interactions of $R_4^4(12)$ ring motif^{15b} in the 5-ASA structure (Figure 8). The Hirshfeld surface 2D fingerprint plot shows the difference between the crystal structures of the neutral and ionic isomers (Figure 9).

2-(*p*-Tolylamino)nicotinic Acid (TNA). TNA was synthesized and crystallized in different organic solvents to obtain three polymorphs.^{6a} The neutral forms were reproducible using normal solvent crystallization techniques and melting methods. But the zwitterionic form, which crystallized previously only in the presence of pyridine type coformers and the separation of zwitterionic form as bulk material, was difficult from the mixture of coformers and concomitant polymorphs.¹³ Thus, comparison of solubility for neutral vs ionic polymorphs could not be conducted for lack of pure polymorphic material. Forms I and II contain the acid–pyridine synthon, whereas Form III has ionic H bonds.^{6a} Other amphoteric compounds chosen for this polymorphic study comparison are 2-phenylaminonicotinic acid (PNA), 2-(*o*-tolylamino)nicotinic acid (*o*-TNA), 4-aminobenzoic acid (PABA). But we were unsuccessful in obtaining neutral and zwitterionic crystal structures for these compounds.

Our studies continued with the structurally similar niflumic acid. Attempts to crystallize neutral and zwitterionic forms of niflumic acid by solvent evaporation and heating techniques gave the neutral form of niflumic acid only. A new Form II recently identified by PXRD^{7g} appears to be very close to the known neutral Form I by IR spectroscopy, and hence it is unlikely to be a zwitterionic structure.

ΔpK_a Calculation for Ampholytes. pK_a values were calculated for all the molecules to know the ΔpK_a rule validity ($\Delta pK_a = pK_a \text{ BaseH}^+ - pK_a \text{ Acid}$) for intramolecular proton transfer in the solid-state for these amphoteric compounds. Recently, Cruz-Cabeza¹⁹ studied the ΔpK_a rule for 6465 multicomponent systems in the CSD and concluded that

ionized acid–base complexes are detected exclusively for $\Delta pK_a > 4$ and nonionized species for $\Delta pK_a < -1$, with only a few exceptions. For acid–base complexes whose ΔpK_a is between -1 to 4 , which is the majority category for organic acid–base complexes and amphoteric molecules, a linear relationship between the probability of salt formation and the pK_a difference was noted. The calculated ΔpK_a values for amphoteric molecules (Table 3) were compared with the observed proton state in the crystal structure. $\Delta pK_a < -2$ for aminobenzoic acids 2-ABA and 3-ABA, and $\Delta pK_a > 3.5$ for aminonicotinic acids (TNA and CLX), $\Delta pK_a = -1.4$ and -1.7 for zwitterionic 5-ASA and torsemide drugs, and 3.8 and 2.9 for 4-ASA and ciprofloxacin and norfloxacin. There seems to be no particular trend here for neutral vs zwitterionic structure and ΔpK_a for amphoteric drug molecules, in what is perhaps the first systematic analysis of this issue.

Characterization of Neutral and Zwitterionic Polymorphs. **PXRD.** Neutral and zwitterionic polymorphs of 2-ABA, 3-ABA, and CLX were characterized for bulk purity by PXRD.²⁰ The calculated powder pattern from the X-ray crystal structure of these polymorphs matched with the experimental powder X-ray line profile (Figure 10).

Solid State NMR. Solid state ¹³C NMR is a powerful technique to identify neutral and zwitterionic polymorphs, for example, of 2-ABA and 3-ABA.^{6,7} The neutral forms of clonixin were characterized by ss-NMR.²¹ The chemical shift of the carboxylic acid carbon of anthranilic acid (2-ABA) and 3-ABA showed significant difference between the neutral and zwitterionic forms. The chemical shift value of COOH for 2-ABA (Form I, half zwitterionic, 172.76 ppm) is shifted upfield compared to the neutral Forms II and III (174.35 and 174.16 ppm), as would be expected from the higher electron density present on the carboxylate group. The upfield drift in the chemical shift of C1 in Form I (149.13 ppm) compared to Form II (152.58 ppm) and III (152.26 ppm) may be due to

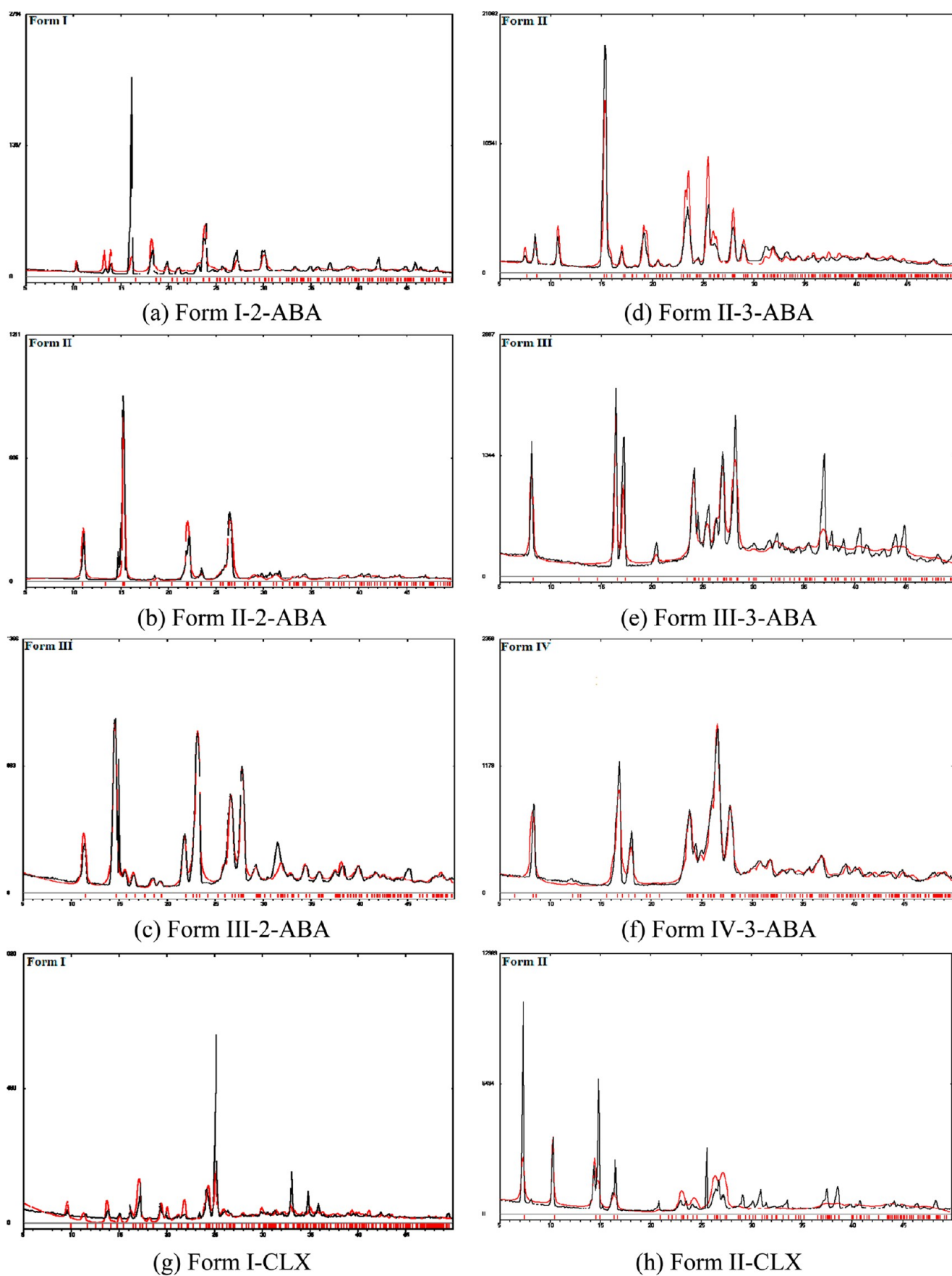


Figure 10. continued

Figure 10. continued

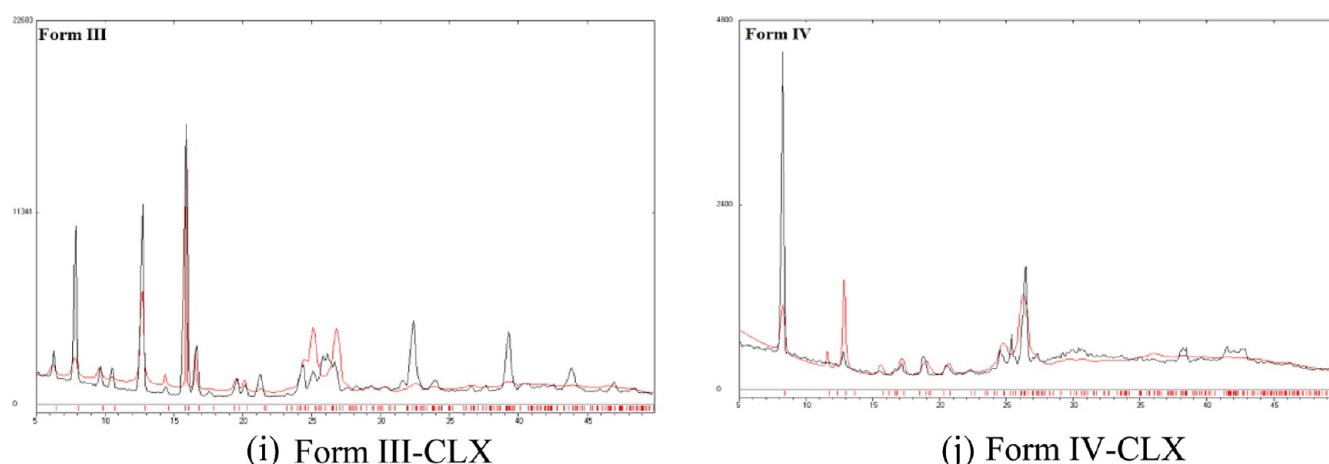


Figure 10. (a–j) Overlay of experimental (black) and calculated (red) powder X-ray line pattern of polymorphs.

electron delocalization at the carboxylate group in the zwitterionic forms (see Figure 11).

The chemical shift values of Form III (172.7 ppm), Form IV (172.1 ppm), and Form II (172.75 ppm) are very close for 3-ABA, and a reason may be the meta-effect of the electron-donating amino group. The chemical shift of C1 in Form III (136.54 ppm) and IV (136.23 ppm) is upfield because of electron delocalization in the carboxylate group compared to the Form II (147.29 ppm). The ss-NMR of clonixin Form II could not be recorded for comparison because of limited sample and difficulty to crystallize the zwitterionic Form II (see Figure S1, Supporting Information). The chemical shift values for all polymorphs are listed (Table S2, Supporting Information).

FT-IR. FT-IR technique has been used to differentiate neutral and zwitterionic polymorphs of ampholytes.^{20,22} For example, the stretching frequency of the carbonyl group in the zwitterionic form (Form I, half zwitterionic, 1636.0 cm⁻¹) of anthranilic acid (2-ABA) is less than that of the other two neutral forms (Form II, neutral, 1652.3 cm⁻¹; Form III, neutral, 1640.0 cm⁻¹). The decrease in the stretching frequency of zwitterionic form is a result of delocalization of electron cloud over the carboxylate group, for example, also in the zwitterionic structure of *m*-aminobenzoic acid (3-ABA). The stretching frequency of the C=O group in carboxylic acid in two zwitterionic polymorphs (Form III and IV, 1622.2, 1629.4 cm⁻¹) is less than that of the reported neutral form (1637.8 cm⁻¹). Similarly clonixin showed a difference between the neutral and zwitterionic polymorphs (Form II, zwitterionic, 1646.7 cm⁻¹; Form I, III, neutral, 1677.3 and 1665.8 cm⁻¹). The fourth form of clonixin showed a broad peak in the FT-IR (not discussed). FT-IR and Raman spectral values are displayed in Figures S2 and S3 and Tables S3 and S4, Supporting Information.

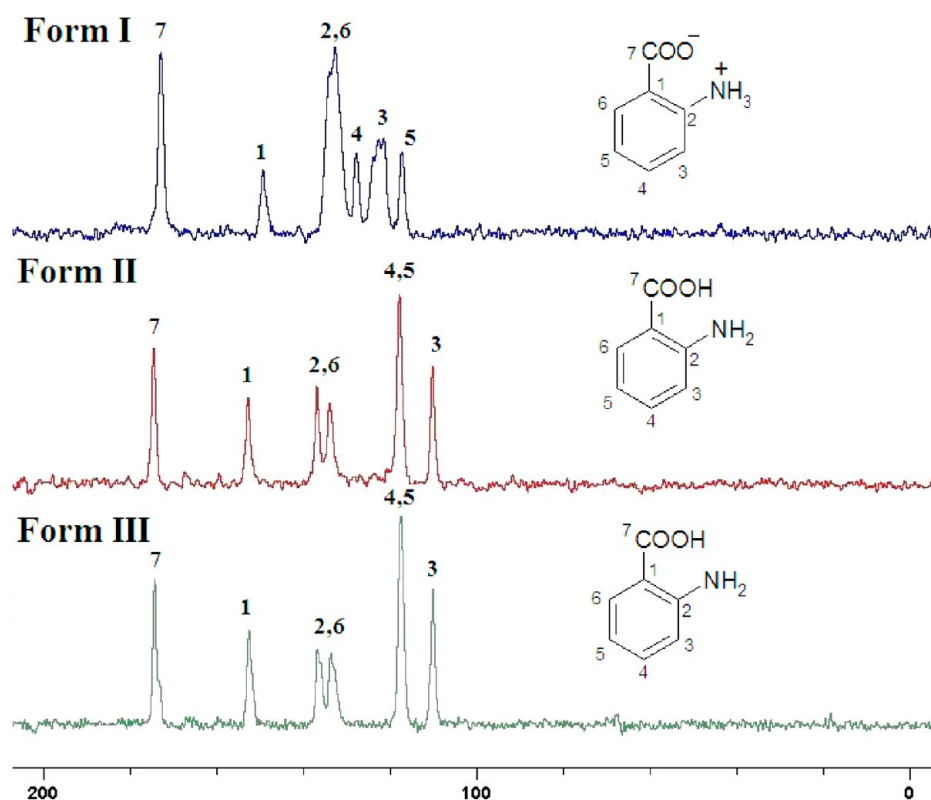
Thermal Stability and Phase Transition Study. The neutral and zwitterionic forms of three ampholyte molecules exhibited extensive phase transitions by DSC and VT-PXRD.²³ The zwitterionic polymorph of 2-ABA transformed to neutral the Form III at 95.9 °C and finally melted at 144 °C. The zwitterionic form and the neutral forms are enantiotropic, with Form I being the low temperature phase and Form III is the high temperature phase. DSC and VT-PXRD for such phase

transitions between neutral and zwitterionic forms of anthranilic acid are displayed in Figure 12. Form I is stable up to 24 h of slurry grinding in aqueous medium, but Forms II and III transformed to Form I in those slurry conditions.^{6d} Our thermal analysis is consistent with the study of Ojala and Etter^{7b} on 2-ABA polymorphs.

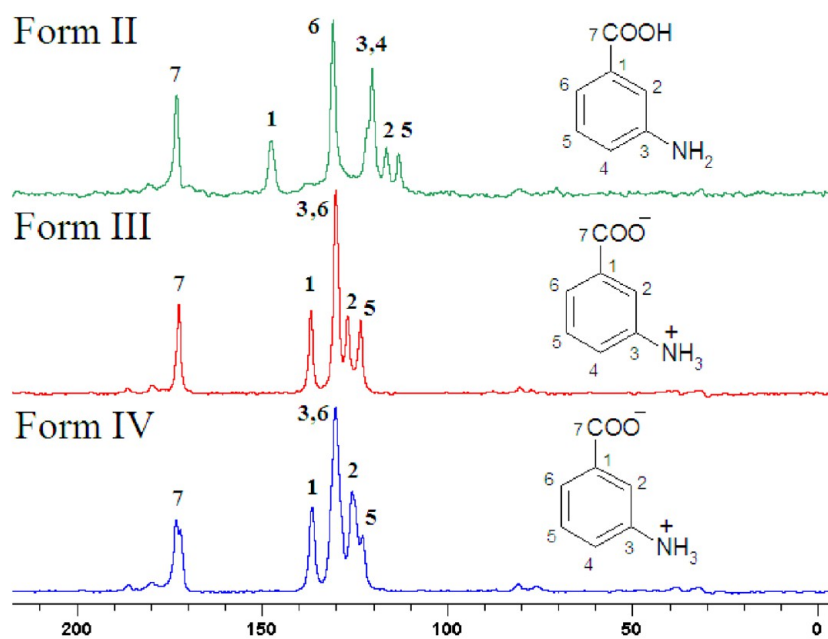
The zwitterionic Form III of *m*-aminobenzoic acid (3-ABA) transformed to another second zwitterionic Form IV at 161.9 °C and melts at 177.1 °C. VT-PXRD suggested that the transformation of zwitterionic Form III to Form IV occurred via neutral Form I as an intermediate phase (Figure 13b), based on PXRD match with the diffraction lines for reported Form I. The zwitterionic Form IV transformed to the neutral Form II at 166.7 °C and then melted at 176.4 °C. We identified Form III as the lower temperature phase and Form II as the higher temperature phase in this study. Form II is unstable at room temperature transformed to the stable Form III. Our measurements qualify the studies of Harris et al.^{6b} wherein they reported III and IV as stable based on the DSC and the density rule. We confirmed zwitterionic Form III as the stable polymorph by slurry experiments (Figure S4, Supporting Information). Forms III and Form IV are enantiotropically related to Form II as reported a previous work^{6b} (Figure 13).

For clonixin (CLX) tetramorphs, the zwitterionic Form II first transformed to Form I at 149.2 °C and then melted at 233.6 °C. Form III underwent a phase transition at 142.4 °C and melted at 233.6 °C. Form II and Form III are enantiotropically related to Form I (see DSC and VT-PXRD in Figure 14). The zwitterionic forms transform to the neutral polymorph upon heating for the above-mentioned three molecules. These data are summarized in Table 4.

Solubility and Dissolution Study. The main motivation of this study was to compare the dissolution rate and solubility of zwitterionic and neutral polymorphs and make structure–solubility correlations. The solubility of 2-ABA, 3-ABA, and CLX polymorphs is tabulated (Table S5). Generally, metastable polymorphs exhibit a higher solubility and dissolution rate compared to the stable form, in line with the inverse solubility–stability trend.^{2,24} Among neutral and zwitterionic polymorphic sets, we observed that the solubility of the zwitterionic form was higher, even when it is the more stable modification compared to the neutral form. In effect, a zwitterionic form can



(a) 2-ABA

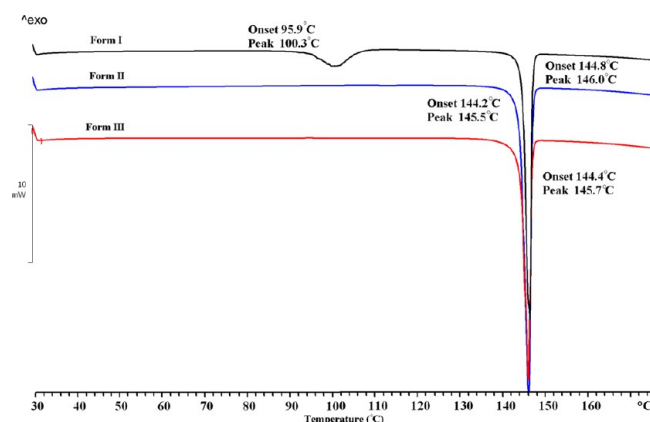


(b) 3-ABA

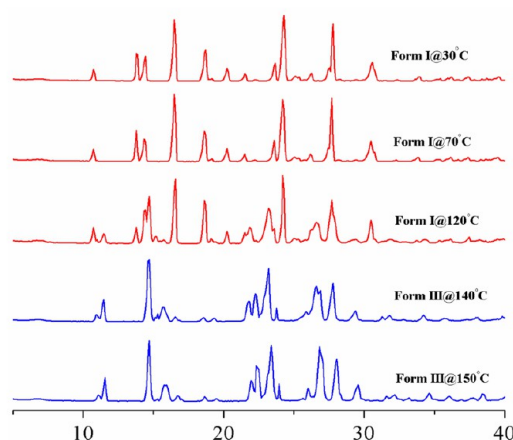
Figure 11. ^{13}C ss-NMR spectra of polymorphs of molecules (a) 2-ABA and (b) 3-ABA.

combine the twin criteria of high solubility and good stability in the same crystalline polymorph, which is a desirable optimization in pharmaceutical development. The reason for the higher solubility is that the ionic functional groups in the zwitterionic crystal structure expose the charged ends of the functional groups to the water and polar solvents; for example, the

charged acidic/basic groups are able to hydrogen bond better with water and alcohol-like solvents. Among the structures studied, the stable form of 2-ABA is half zwitterionic/neutral (Form I), and its solubility is higher (10.33 mg/mL) than the neutral forms (Form II; 6.37 mg/mL, Form III; 3.97 mg/mL) in water medium. The stability of Form I was confirmed in a



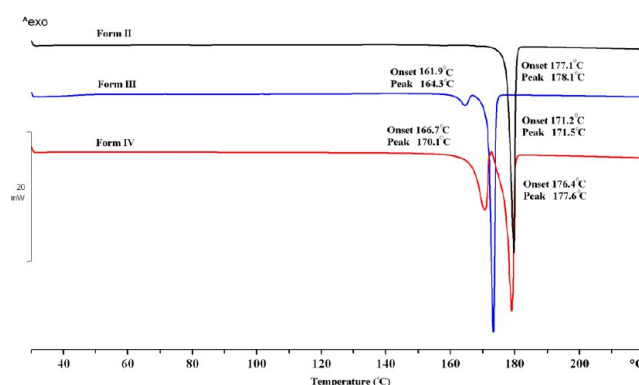
(a) DSC of 2-ABA



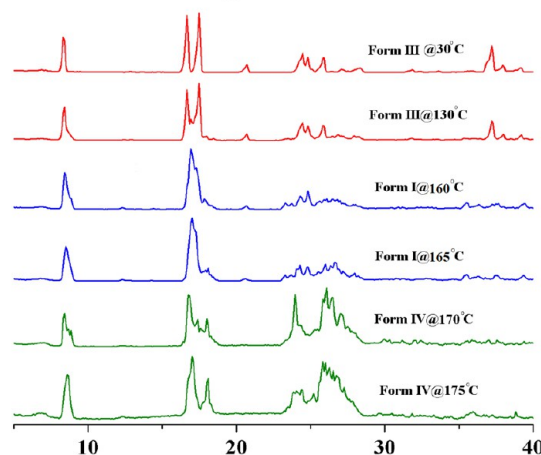
(b) VT-PXRD-Form I, 2-ABA

Figure 12. (a) Thermal analysis by DSC and (b) VT-PXRD shows the phase transition of neutral and zwitterionic Form I to Form III of 2-ABA at 120 °C.

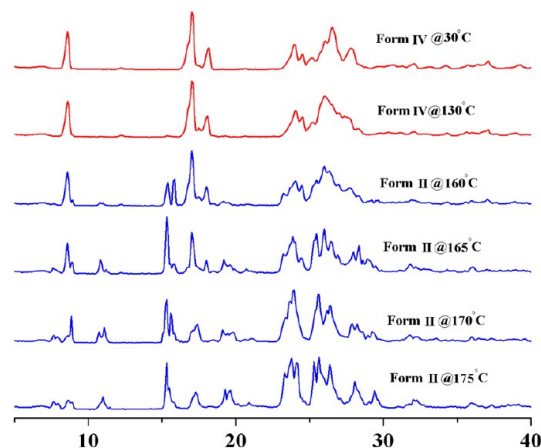
slurry experiment at ambient conditions, and there was no interconversion to the neutral forms after 24 h. The neutral Forms II and Form III of 2-ABA transformed to the stable ionic Form I under the same slurry conditions. The density and packing fraction of Form I (1.40 g cm^{-3} , 72.4%) is greater than Form II (1.37 g cm^{-3} , 68.5%) and Form III (1.39 g cm^{-3} , 70.2%), consistent with the observed stability order. The solubility trends for 3-ABA in water is Form IV (zwitterionic, most stable) 7.69 mg/mL > Form III 6.07 mg/mL (zwitterionic) > Form II 4.34 mg/mL (neutral; least stable). The density and packing fraction of zwitterionic Form III (1.55 g/cm^3 , 78.2%) and Form IV (1.53 g/cm^3 , 77.1%) of 3-ABA are higher than that of neutral Form II (1.37 g/cm^3 , 69.6%). That the zwitterionic form is more stable than the neutral form was confirmed in slurry experiments over 24 h. For CLX, the solubility of metastable forms III and IV is higher than that of the ionic stable forms in 60% EtOH–water mixture. The solubility of zwitterionic Form II (2.01 mg/mL) is slightly higher than the stable neutral Form I (1.93 mg/mL) for CLX. The higher solubility of the zwitterionic forms is similar to the solubility trend followed in aminobenzoic acid polymorphs and varies inversely with crystal density and packing fraction (Form I: 1.41 g/cm^3 , 67.8%; Form II: 1.51 g/cm^3 , 72.8%). The apparent solubility of neutral, metastable polymorphs of CLX, Forms III and IV (2.32 mg/mL and 2.25 mg/mL), is higher than that of stable Form I and



(a) DSC of 3-ABA



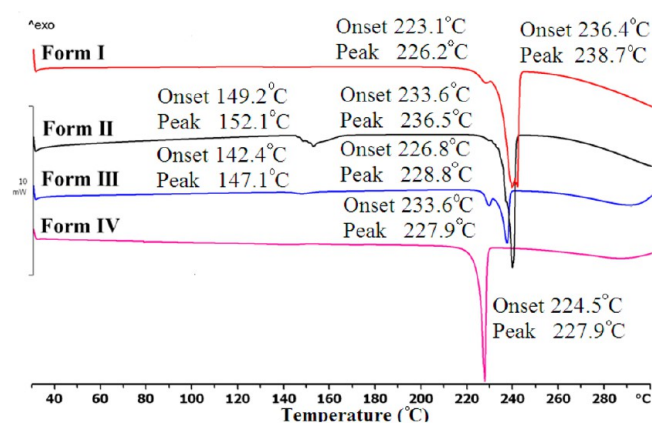
(b) VT-PXRD of form III of 3-ABA



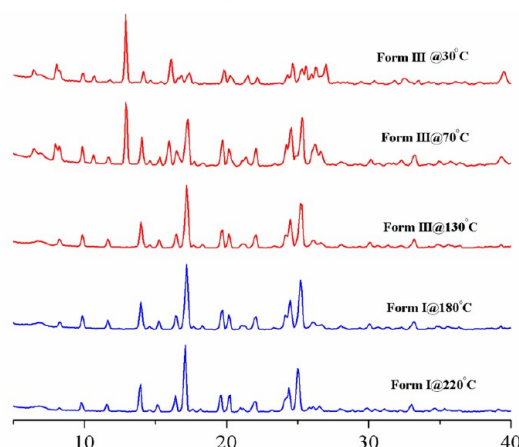
(c) VT-PXRD of form IV of 3-ABA

Figure 13. Thermal behavior of 3-ABA trimorphs. (a) DSC; (b) Form III to Form I at 160 °C, and Form I to Form IV at 165 °C; and (c) Form IV to Form II at 160 °C by VT-PXRD.

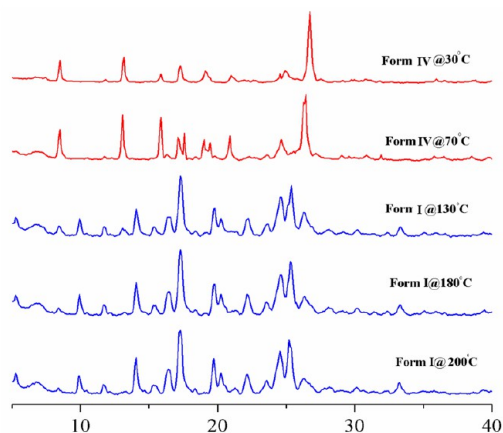
zwitterionic Form II (1.93 mg/mL and 2.01 mg/mL). The solubility of these two metastable forms is not consistent with their higher crystal density and packing efficiency (Form III 1.51 g cm^{-3} , 72.7%; Form IV 1.49 g cm^{-3} , 71.6%). The higher density perhaps arises from the planar conformation in these metastable polymorphs III and IV, which results in a denser packing of molecules. Even though we recently concluded that planar a molecular conformation tends to give low solubility,¹⁸ the present results appear to be an oddity with the planar conformation and higher density polymorphs III and IV of CLX exhibiting higher solubility. The neutral forms III and IV of



(a) DSC of CLX



(b) VT-PXRD of form III of CLX



(c) VT-PXRD of form IV of CLX

Figure 14. Thermal behavior of tetramorphs of clonixin by (a) DSC, (b) Form III to Form I at 130 °C, and (c) Form IV to Form I at 130 °C by VT-PXRD.

Table 4. Thermodynamic Parameters of Polymorphic Systems

molecule	2-aminobenzoic acid			3-aminobenzoic acid			clonixin			
polymorph	Form I	Form II	Form III	Form II	Form III	Form IV	Form I	Form II	Form III	Form IV
melting and phase transition onset	95.9	144.2	144.4	177.1	161.9	166.7	236.4	149.2	142.4	224.4
enthalpy of fusion/enthalpy of transition (kJ mol ⁻¹)	23.6, 5.4	23.4	22.9	28.8	30.2, 1.8	21.0, 10.8	27.1	29.9, 5.8	21.2, 1.5	21.2
density (g cm ⁻³)	1.40	1.37	1.39	1.37	1.55	1.53	1.41	1.51	1.51	1.49
packing fraction (%)	72.4	68.5	70.2	69.6	78.2	77.1	67.8	72.8	72.7	71.6
thermodynamic relationship and stable polymorph	enantiotropic and stable half-zwitterionic Form I			enantiotropic and stable zwitterionic Form III			enantiotropic and stable neutral/ionic Form I ≈ II			

Table 5. Solubility and Dissolution Rate of Polymorphs

polymorph	nature in solid state	absorption coefficient (ε), (M ⁻¹ cm ⁻¹)	solubility (mg/mL)	intrinsic dissolution rate (mg/cm ²)
2-Aminobenzoic Acid Polymorphs				
Form I	half zwitterionic/neutral	12.26	10.33	1.36
				1.75
Form II	neutral	13.60	9.25	0.82
			6.37 ^a	0.93
Form III	neutral	12.39	8.01	0.67
			3.97 ^a	
3-Aminobenzoic Acid Polymorphs				
Form II	neutral	6.22	7.81	0.84
			4.34 ^a	
Form III	zwitterionic	6.22	6.07	1.51
Form IV	zwitterionic	6.25	7.69	1.56
Clonixin Polymorphs				
Form I	neutral	68.36	1.93	0.14
Form II	zwitterionic	69.27	2.01	0.20
Form III	neutral	57.58	3.12	0.19
			2.32 ^a	
Form IV	neutral ^b	98.36	2.51	0.16
			2.25 ^a	
Aminosalicic Acid Isomers				
4-ASA	neutral	60.49	2.54 ^c	0.25
5-ASA	zwitterionic	22.32	1.43 ^c	0.17

^aFor these metastable forms the apparent solubility was measured.

^bThe neutral nature of COOH was derived from the C=O, C–O distances (1.23 Å, 1.31 Å) in .cif file BIXGIY03. ^cSolubility is reported in ref 12g,h. The compound suffered degradation in long-term solubility experiments (24 h).

CLX transformed to the stable neutral Form I in slurry experiments, whereas zwitterionic Form II and neutral Form I are stable to the same aqueous solution (Figure S5, Supporting Information).

The dissolution rates of zwitterionic forms of 2-ABA, 3-ABA, and CLX are higher than the neutral forms (Table 5 and Figure 15). The IDR of zwitterionic Form I of 2-ABA is 1.36 mg/cm², and it dissolves faster than the neutral forms (Form II 0.82 mg/cm², Form III 0.67 mg/cm²). The dissolution rate of Form III (1.51 mg/cm²) and Form IV (1.56 mg/cm²) is almost two times faster than that of neutral Form II for 3-ABA. The dissolution rate of zwitterionic Form II (0.20 mg/cm²) of CLX is higher than that of neutral polymorphs I (0.14 mg/cm²) and III (0.19 mg/cm²) and IV (0.16 mg/cm²).

The dissolution rate of the two isomers of aminosalicic acid was compared to compare the solubility difference between the ionic and neutral isomers of APIs. The neutral structure of 4-ASA exhibited higher dissolution rate than the zwitterionic structure of 5-ASA. The density and melting point of 5-ASA

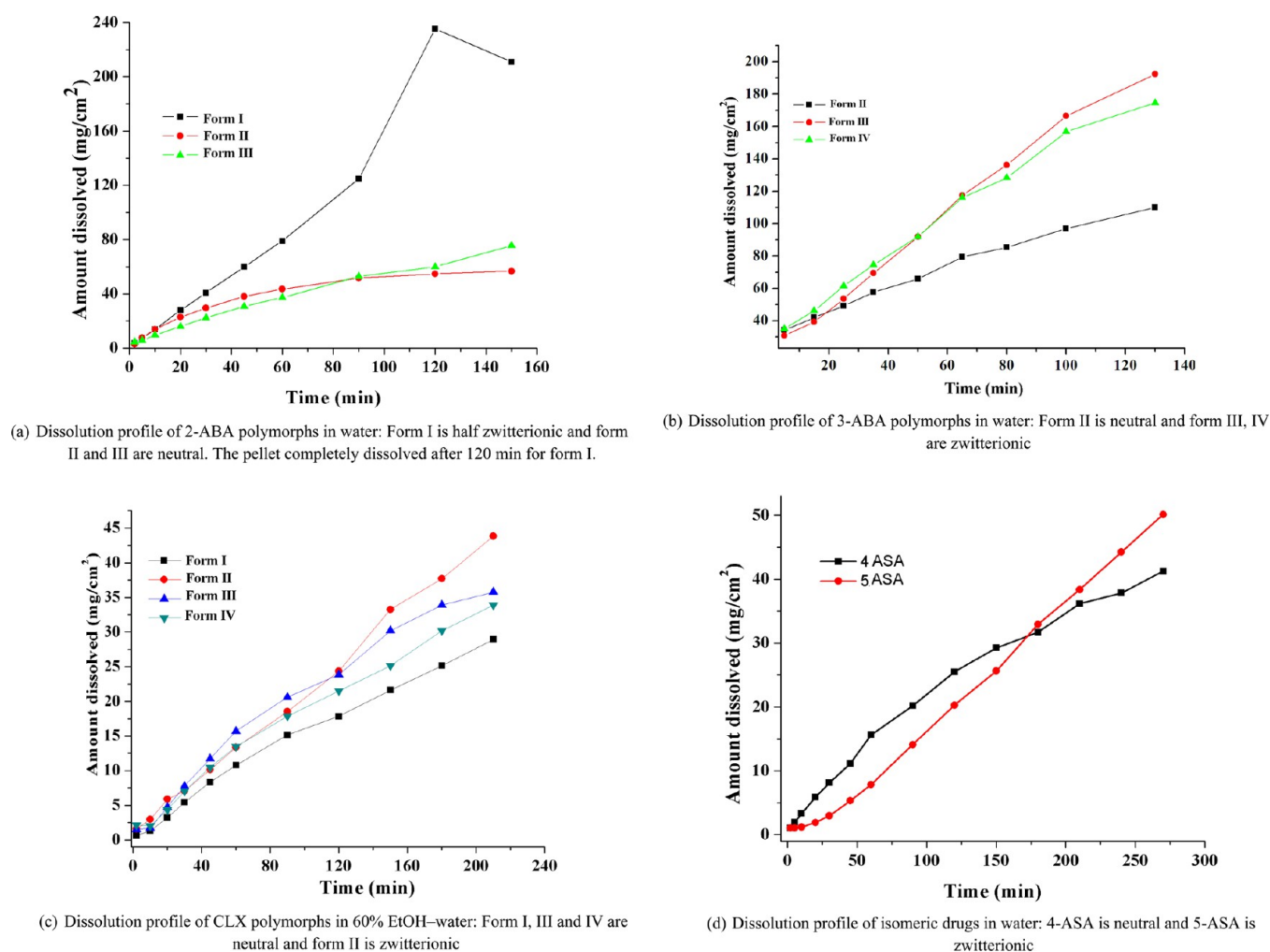


Figure 15. (a–d) Dissolution profiles of neutral and zwitterionic crystalline drugs at 30 °C.

(mp 283 °C, D_c 1.56 g cm⁻³) are higher than that for 4-ASA (mp 150 °C, D_c 1.48 g cm⁻³), and the lower solubility of zwitterionic 5-ASA with strong ionic N⁺–H...O⁻ hydrogen bonds is again counterintuitive. In any case, these isomeric structures are not truly polymorphic but have similar molecular structures.

CONCLUSIONS

Several drugs are amphoteric in nature. This structural-cum-solubility study of neutral and zwitterionic polymorphs provides methods for their preparation and a comparison of solubility–stability characteristics. Normally solubility and stability are inversely related for drug polymorphs. We show that the twin characteristics of high solubility and good stability may be jointly optimized in the same zwitterionic polymorph for amphoteric drugs. The high polarity and ionic nature of acidic/basic groups promote hydrogen bonding with water (for higher solubility) as well as a tighter crystal lattice of ionized molecules (polymorph stability). All the crystal structures were fully characterized by FT-IR, Raman and ss-NMR as well as PXRD line pattern. The thermodynamic relationships and phase transition between the neutral and zwitterionic polymorphs were analyzed by DSC and VT-PXRD. This study provides a new direction to crystallize ionic polymorphs of amphoteric drugs for solubility enhancement. The selective crystallization of zwitterionic forms could be possible through crystallization

promoter additives such as ionic liquids,²⁵ polymer-induced heteronucleation,²⁶ and seeding with ionic structural mimics.²⁷

EXPERIMENTAL SECTION

General. 2-ABA, 3-ABA, 4-ASA, 5-ASA, and NFA were purchased from Sigma-Aldrich, Hyderabad, India. All other solvents, reagents, and cofomers were purchased from commercial sources and used without further purification.

Synthesis. Clonixin, PNA, *o*-TNA, and *p*-TNA were synthesized by refluxing *o*-chloronicotinic acid (315.3 mg, 2 mmol) and an equivalent amount of the appropriate aromatic amine (1.1 equiv). The precipitated product was filtered and purified by crystallization from acetone to obtain pure clonixin (CLX), 2-(phenylamino)nicotinic acid, 2-(*o*-tolylamino)nicotinic acid, and 2-(*p*-tolylamino)nicotinic acid which were characterized by NMR and single crystal XRD.

Vibrational Spectroscopy. Nicolet 6700 FT-IR spectrometer with an NXR FT-Raman module was used to record IR spectra. IR spectra were recorded on samples dispersed in KBr pellet.

CSD Search. A search of the CSD (version 5.34, November 2012)¹⁴ was performed by drawing the amine and the acid groups as search criteria all organic compounds with the word “form”, “polymorph”, “modification”, and “phase” in the qualifier, excluding the entries for which 3D coordinates are not available. These searches resulted in only four drugs and three model compounds having zwitterionic and neutral polymorphic sets for single component organic molecules with solved X-ray crystal structures. Another search on amino acids gave 223 hits, but only eight zwitterionic polymorphs

of amino acids resulted from this search. There are no neutral–zwitterionic polymorph sets for amino acids at the present time in the CSD.

¹³C ss-NMR Spectroscopy. Solid state NMR spectra were recorded on a Bruker Advance spectrometer operating at 400 MHz (100 MHz for ¹³C nucleus). ss-NMR spectra were recorded on a Bruker 4 mm double resonance CP-MAS probe in zirconia rotors at 5.0 kHz spin rate with a cross-polarization contact time of 2.5 ms and a recycle delay of 8 s. ¹³C CP-MAS spectra recorded at 100 MHz were referenced to the methylene carbon of glycine, and then the chemical shifts were recalculated to the TMS scale ($\delta_{\text{glycine}} = 43.3$ ppm).

Thermal Analysis. DSC was performed on Mettler Toledo DSC 822e module. Samples were placed in crimped but vented aluminum sample pans. The typical sample size was 3–4 mg, and the temperature range was 30–250 °C at heating rate of 5 °C/min. Samples were purged by a stream of dry nitrogen flowing at 150 mL/min.

Dissolution and Solubility Measurements. Intrinsic dissolution rate (IDR) and solubility measurements were carried out on a USP certified Electrolab TDT-08 L dissolution tester (Electrolab, Mumbai, MH, India). A calibration curve was obtained for all aminobenzoic acids molecules and its polymorphs by plotting absorbance vs concentration UV–vis spectra curves on a Thermo Scientific Evolution EV300 UV–vis spectrometer (Waltham, MA) for known concentration solutions in water and 60% EtOH–water medium. The mixed solvent system (EtOH–water) was selected for its higher solubility of CLX polymorphs in this medium. The slope of the plot from the standard curve gave the molar extinction coefficient (ϵ) by applying the Beer–Lambert's law. Equilibrium solubility was determined in water for 2-ABA, 3-ABA, and salicylic acids and 60% EtOH–water medium for CLX polymorphs using the shake-flask method. To obtain equilibrium solubility, 100 mg of each solid material was stirred for 24 h in 5 mL of water for ABA polymorphs and 60% EtOH–water for CLX polymorphs at 37 °C, and the absorbance was measured at 318 and 327 nm for 2-ABA and 3-ABA polymorphs, and 289 nm for CLX polymorphs. The concentration of the saturated solution was calculated at 24 h, which is referred to as the equilibrium solubility of the stable solid form. The dissolution rates are obtained from the IDR experiments.

Powder X-ray Diffraction. PXRDs were recorded on a SMART Bruker D8 Advance X-ray diffractometer (Bruker-AXS, Karlsruhe, Germany) in the Bragg–Brentano geometry using Cu K α X-ray radiation ($\lambda = 1.5406$ Å) at 40 kV and 30 mA. Diffraction patterns were collected over the 2θ range of 5–50° at a scan rate of 1°/min. The appearance of polymorphs for all the molecules was monitored by the appearance of new diffraction peaks. Powder Cell 2.359²⁸ was used for overlaying the experimental PXRD pattern on the calculated lines from the crystal structure. Variable temperature mode fixed on the same instrument and recorded the phase transition with 600–1200 s delay time at a heating rate of 2 °C/min.

pK_a Calculation. pK_a values were calculated using ChemAxon software for all the ampholytes. These values are calculated theoretically in aqueous medium. This software is available free of charge on this Web site <http://www.chemaxon.com> as Marvin 6.0.1, 2013, ChemAxon software.

■ ASSOCIATED CONTENT

■ Supporting Information

Figure S1: ¹³C ss-NMR spectra of CLX polymorphs. Figure S2: FT-IR comparison of polymorphs for 2-ABA, 3-ABA, and CLX. Figure S3: FT-Raman comparison of polymorphs for 2-ABA, 3-ABA, and CLX. Figure S4: PXRD line pattern of form I, form II, form III of 2-ABA, form II, form III, form IV of 3-ABA, and form I, form III, form IV of CLX. Figure S5: FT-IR of form II. Table S1: List of amphoteric drugs in the market. Table S2: Chemical shift values for polymorphs. Table S3: FT-IR stretching frequencies for polymorphs. Table S4: Raman stretching frequencies for polymorphs. This material is available free of charge via the Internet at <http://pubs.acs.org>.

■ AUTHOR INFORMATION

Corresponding Author

*E-mail ashwini.nangia@gmail.com.

Notes

The authors declare no competing financial interest.

■ ACKNOWLEDGMENTS

This research was funded by J. C. Bose fellowship (DST-SERB scheme SR/S2/JCB-06/2009), and Novel solid-state forms of APIs (SERB scheme SR/S1/OC-37/2011). DST (IRPHA) and University Grants Commission (UGC-PURSE grant) are thanked for providing instrumentation and infrastructure facilities. S.S.K. thanks the CSIR for a research fellowship.

■ REFERENCES

- (1) (a) López-Mejías, V.; Kampf, J.; Matzger, A. *J. Am. Chem. Soc.* **2012**, *134*, 9872. (b) Halebian, J.; McCrone, W. *J. Pharm. Sci.* **2006**, *58*, 911. (c) Byrn, S. R.; Pfeiffer, R. R.; Stowell, J. G. *Solid-State Chemistry of Drugs*, 2nd ed.; SSCI Inc.: West Lafayette, 1999. (d) Dunitz, J.; Gavezzotti, A. *J. Phys. Chem. B* **2012**, *116*, 6740. (e) Allen, K.; Davey, R. J.; Ferrari, E.; Towler, C.; Tiddy, G. J. T.; Jones, M.; Pritchard, R. G. *Cryst. Growth Des.* **2002**, *2*, 523. (f) Kitamura, M. *CrystEngComm* **2009**, *11*, 949. (g) Allen, F. H. *Acta. Crystallogr., Sect. B* **2002**, *B58*, 380. (h) Grant, D. J. W. *Polymorphism in Pharmaceutical Solids*; Brittain, H. G., Ed.; Marcel Dekker Inc.: New York, 1999; pp 1–32. (i) Mullin, J. W. *Crystallization*, 4th ed.; Butterworth-Heinemann: Oxford, U.K., 2001. (j) McCrone, W. C. *Polymorphism in Physics and Chemistry of the Organic Solid-State*; Fox, D., Labes, M. M., Weissberger, A., Eds.; Wiley-Interscience: New York, 1965; Vol. 2, p 725. (k) Braga, D.; Grepioni, F. *Making Crystals by Design*; John-Wiley: New York, 2007; p 348.
- (2) (a) Maher, A.; Rasmuson, Å. C.; Croker, D. M.; Hodnett, B. K. *J. Chem. Eng. Data* **2012**, *57*, 3525. (b) Bartolomei, M.; Bertocchi, P.; Ramusino, M. C.; Santucci, N.; Valvo, L. *J. Pharm. Biomed. Anal.* **1999**, *21*, 299. (c) Avdeef, A. *Solubility, in Absorption and Drug Development: Solubility, Permeability, and Charge State*, 2nd ed.; John-Wiley: New York, 2012; p 251. (d) Lipinski, C.; Lombardo, F.; Dominy, B.; Feeney, P. *Adv. Drug Delivery Rev.* **2001**, *46*, 3. (e) Lipinski, C. *J. Pharmacol. Toxicol. Methods* **2000**, *44*, 235. (f) Urakami, K.; Shono, Y.; Higashi, A.; Umemoto, K.; Godo, M. *Bull. Chem. Soc. Jpn.* **2002**, *75*, 1241. (g) Abramov, Y. A.; Pencheva, K. *Thermodynamics and Relative Solubility Prediction of Polymorphic Systems, In Chemical Engineering in the Pharmaceutical Industry: R&D to Manufacturing*; am Ende, D. J., Ed.; John-Wiley: New York, 2010; p 477.
- (3) (a) Bauer, J.; Spanton, S.; Henry, R.; Quick, J.; Dziki, W.; Porter, W.; Morris, J. *J. Pharm. Res.* **2001**, *18*, 859. (b) Sanphui, P.; Sarma, B.; Nangia, A. *J. Pharm. Sci.* **2011**, *100*, 2287. (c) Cherukuvada, S.; Thakuria, R.; Nangia, A. *Cryst. Growth Des.* **2010**, *10*, 3931. (d) Johnson, S. R.; Chen, X.-Q.; Murphy, D.; Gudmundsson, O. *Mol. Pharmaceutics* **2007**, *4*, 513. (e) Lalit, R.; Sanphui, P.; Desiraju, G. R. *Cryst. Growth. Des.* **2010**, *13*, 3681.
- (4) (a) Babu, N. J.; Nangia, A. *Cryst. Growth Des.* **2011**, *11*, 2662. (b) Serajuddin, A. *Adv. Drug Delivery Rev.* **2007**, *59*, 603. (c) Llinàs, A.; Glen, R. C.; Goodman, J. M. *J. Chem. Inf. Model.* **2008**, *48*, 1289. (d) Alsenz, J.; Kansy, M. *Adv. Drug Delivery Rev.* **2007**, *59*, 546. (e) Giron, D. *Thermochim. Acta* **1995**, *248*, 1.
- (5) (a) Bordallo, H.; Boldyreva, E.; Buchsteiner, A.; Koza, M.; Landsessel, S. *J. Phys. Chem. B* **2008**, *112*, 8748. (b) Hamilton, B. D.; Hillmyer, M. A.; Ward, M. D. *Cryst. Growth Des.* **2008**, *8*, 3368. (c) Huang, J.; Yu, L. *J. Am. Chem. Soc.* **2006**, *128*, 1873. (d) Moggach, S. A.; Parsons, S.; Wood, P. A. *Cryst. Rev.* **2008**, *14*, 143. (e) Jámroz, M.; Rode, J.; Ostrowski, S.; Lipiński, P.; Dobrowolski, J. *J. Chem. Inf. Model.* **2012**, *52*, 1462. (f) Luker, T.; Bonnert, R.; Paine, S.; Schmidt, J.; Sargent, C.; Cook, A.; Cook, A.; Gardiner, P.; Hill, S.; Weyman-Jones, C. *J. Med. Chem.* **2011**, *54*, 1779. (g) Flaig, R.; Koritsanszky, T.; Ditttrich, B.; Wagner, A.; Luger, P. *J. Am. Chem. Soc.* **2002**, *124*, 3407.

- (6) (a) Nath, N. K.; Kumar, S. S.; Nangia, A. *Cryst. Growth Des.* **2011**, *11*, 4594. (b) Williams, P. A.; Hughes, C. E.; Lim, G. K.; Kariuki, B. M.; Harris, K. D. M. *Cryst. Growth Des.* **2012**, *12*, 3104. (c) Orola, L.; Veidis, M.; Sarcevic, I.; Actins, A.; Belyakov, S.; Platonenko, A. *Int. J. Pharm.* **2012**, *432*, 50. (d) Trask, A.; Shan, N.; Motherwell, W.; Jones, W.; Feng, S.; Tan, R.; Carpenter, K. *Chem. Commun.* **2005**, 880. (e) Takasuka, M.; Nakai, H.; Shiro, M. *J. Chem. Soc., Perkin Trans. 2* **1982**, 1061. (f) Long, S.; Parkin, S.; Siegler, M. A.; Cammers, A.; Li, T. *Cryst. Growth Des.* **2008**, *8*, 4006. (g) Long, S.; Li, T. *Cryst. Growth Des.* **2009**, *9*, 4993. (h) Mahapatra, S.; Venugopala, K. N.; Row, T. N. G. *Cryst. Growth Des.* **2010**, *10*, 1866. (i) Fabbiani, F. P. A.; Ditttrich, B.; Florence, A. J.; Gelbrich, T.; Hursthouse, M. B.; Kuhs, W. F.; Shankland, N.; Sowa, H. *CrystEngComm* **2009**, *11*, 1396.
- (7) (a) Hardy, G. E.; Kaska, W. C.; Chandra, B. P.; Zink, J. I. *J. Am. Chem. Soc.* **1981**, *103*, 1074. (b) Ojala, W. H.; Etter, M. C. *J. Am. Chem. Soc.* **1992**, *114*, 10288. (c) Carter, P. W.; Ward, M. D. *J. Am. Chem. Soc.* **1994**, *116*, 769. (d) Brown, C. J.; Ehrenberg, M. *Acta Crystallogr., Sect. C* **1985**, *C41*, 441. (e) Takazawa, H.; Ohba, S.; Saito, Y. *Acta Crystallogr., Sect. C* **1986**, *C42*, 1880. (f) Lu, T. H.; Chattopadhyay, P.; Liao, F. L.; Lo, J. M. *Anal. Sci.* **2001**, *17*, 905. (g) Bag, P.; Reddy, C. M. *Cryst. Growth Des.* **2012**, *12*, 2740. (h) Voogd, J.; Verzijl, B. H. M.; Duisenberg, A. J. M. *Acta Crystallogr., Sect. B* **1980**, *36*, 2805. (i) Svård, M.; Nordström, F. L.; Jasnobulka, T.; Rasmuson, Å. C. *Cryst. Growth Des.* **2010**, *10*, 195. (j) López-Mejías, V.; Kampf, J. W.; Matzger, A. J. *J. Am. Chem. Soc.* **2009**, *131*, 4554. (k) Lee, E. H.; Byrn, S. R.; Carvajal, M. T. *Pharm. Res.* **2006**, *23*, 2375.
- (8) (a) Tam, K.; Avdeef, A.; Tsinman, O.; Sun, N. *J. Med. Chem.* **2010**, *53*, 392. (b) Towler, C.; Davey, R.; Lancaster, R.; Price, C. *J. Am. Chem. Soc.* **2004**, *126*, 13347. (c) Torbeev, V. Y.; Shavit, E.; Weissbuch, I.; Leiserowitz, L.; Lahav, M. *Cryst. Growth Des.* **2005**, *5*, 2190. (d) Srinivasan, K.; Devi, K. R.; Azhagan, S. A. *Cryst. Res. Technol.* **2011**, *46*, 159.
- (9) (a) Varma, M.; Gardner, I.; Steyn, S.; Nkansah, P.; Rotter, C.; Whitney-Pickett, C.; Zhang, H.; Di, L.; Cram, M.; Fenner, K.; El-Kattan, A. *Mol. Pharm.* **2012**, *9*, 1199. (b) Bouchard, G.; Pagliara, A.; Carrupt, P.-A.; Testa, B.; Gobry, V.; Girault, H. *Pharm. Res.* **2002**, *19*, 1150. (c) Sznitowska, M.; Janicki, S.; Gos, T. *Int. J. Pharm.* **1996**, *137*, 125. (d) Avdeef, A. *Curr. Top. Med. Chem.* **2001**, *1*, 277. (e) Pagliara, A.; Carrupt, P.-A.; Caron, G.; Gaillard, P.; Testa, B. *Chem. Rev.* **1997**, *97*, 3385.
- (10) (a) Mazák, K.; Noszál, B. *J. Med. Chem.* **2012**, *55*, 6942. (b) Mazák, K.; Tóth, G.; Kökösi, J.; Noszál, B. *Eur. J. Pharm. Sci.* **2012**, *47*, 921. (c) Tóth, G.; Mazák, K.; Hosztafi, S.; Kökösi, J.; Noszál, B. *J. Pharm. Biomed. Anal.* **2013**, *76*, 112. (d) Okolotowicz, K. J.; Dwyer, M.; Smith, E.; Cashman, J. R. *J. Biochem. Mol. Toxicol.* **2013**, *28*, 23.
- (11) (a) Surov, A. O.; Terekhova, I. V.; Bauer-Brandl, A.; Perlovich, G. L. *Cryst. Growth Des.* **2009**, *9*, 3265. (b) Moser, P.; Sallmann, A.; Wiesenberger, I. *J. Med. Chem.* **1990**, *33*, 2358. (c) Perlovich, G. L.; Surov, A. O.; Hansen, L. K.; Brandl, A. B. *J. Pharm. Sci.* **2007**, *96*, 1031. (d) Hee, E.; Lee, E. H.; Boerrigter, S. X. M.; Byrn, S. R. *Cryst. Growth Des.* **2010**, *10*, 518. (e) Surov, A. O.; Sztern, P.; Zielenkiewicz, W.; Perlovich, G. L. *J. Pharm. Biomed. Anal.* **2009**, *50*, 831.
- (12) (a) Bertinotti, F.; Giacomello, C. *Acta Crystallogr.* **1954**, *7*, 808. (b) Kornblum, S.; Sciarra, B. *J. Pharm. Sci.* **1964**, *53*, 935. (c) Apelblat, A.; Manzurola, E. *J. Chem. Thermodyn.* **1999**, *31*, 869. (d) André, V.; Braga, D.; Grepioni, F.; Duarte, M. T. *Cryst. Growth Des.* **2009**, *9*, 5108. (e) Montis, R.; Hursthouse, M. B. *CrystEngComm* **2012**, *14*, 5242. (f) Banić-Tomišić, Z.; Kojić-Prodić, B.; Širola, J. *Mol. Struct.* **1997**, *416*, 209. (g) Forbes, R. T.; York, P.; Davidson, J. R. *Int. J. Pharm.* **1995**, *126*, 199. (h) French, D. L.; Mauger, J. W. *Pharm. Res.* **1993**, *10*, 1285. (i) Lichtenstein, G. *Gastroenterol. Hepatol.* **2009**, *5*, 65.
- (13) (a) Bernstein, J.; Davey, R. J.; Henck, J. O. *Angew. Chem., Int.* **1999**, *38*, 3441. (b) Munshi, P.; Venugopala, K. N.; Jayashree, B. S.; Row, T. N. G. *Cryst. Growth Des.* **2004**, *4*, 1105. (c) Long, S.; Siegler, M. A.; Mattei, A.; Li, T. *Cryst. Growth Des.* **2011**, *11*, 414. (d) Long, S.; Parkin, S.; Siegler, M.; Brock, C. P.; Cammers, A.; Li, T. *Cryst. Growth Des.* **2008**, *8*, 3137.
- (14) Cambridge Structural Database, ver. 5.34, ConQuest 1.15, November 2012 release, May 2013 update, Cambridge Crystallographic Data Center, www.ccdc.cam.ac.uk.
- (15) (a) Desiraju, G. R. *Chem. Commun.* **1997**, 1475. (b) Etter, M. C. *Acc. Chem. Res.* **1990**, *23*, 120. (c) Desiraju, G. R.; Vittal, J. J.; Ramanan, A. *Crystal Engineering: A Textbook*; World Scientific: Singapore, 2011; p 25.
- (16) (a) McKinnon, J. J.; Spackman, M. A.; Mitchell, A. S. *Acta Crystallogr., Sect. B* **2004**, *B60*, 627. (b) Spackman, M. A.; Jayatilaka, D. *CrystEngComm* **2009**, *11*, 19. (c) Kumar, S. S.; Nangia, A. *CrystEngComm* **2013**, *15*, 6498. (d) Minkov, V. S.; Tumanov, N. A.; Cabrerabc, R. Q.; Boldyreva, E. V. *CrystEngComm* **2010**, *12*, 2551.
- (17) (a) Nangia, A. *Acc. Chem. Res.* **2008**, *41*, 595. (b) Nangia, A. *Models, Mysteries and Magic of Molecules*; Boeyens, J. C. A., Ogilvie, J. F., Eds.; Springer: New York, 2008; p 63.
- (18) Kumar, S. S.; Rana, S.; Nangia, A. *Chem. Asian J.* **2013**, *8*, 1551.
- (19) Cruz-Cabeza, A. J. *CrystEngComm* **2012**, *14*, 6362.
- (20) (a) Minkov, V. S.; Goryainov, S. V.; Boldyreva, E. V.; Görbitz, C. H. *J. Raman Spectrosc.* **2010**, *41*, 1748. (b) Lee, A. Y.; Lee, I. S.; Myerson, A. S. *Chem. Eng. Technol.* **2006**, *29*, 281. (c) Ramachandran, E.; Baskaran, K.; Natarajan, S. *Cryst. Res. Technol.* **2007**, *42*, 73. (d) Sabino, A. S.; Sousa, G. P. D.; Luz-Lima, C.; Freire, P. T. C.; Melo, F. E. A.; Filho, J. *Solid State Commun.* **2009**, *149*, 1553.
- (21) (a) Sheth, A. R.; Lubach, J. W.; Munson, E. J.; Muller, F. X.; Grant, D. J. W. *J. Am. Chem. Soc.* **2005**, *127*, 6641. (b) Chierotti, M. R.; Ferrero, L.; Garino, N.; Gobetto, R.; Pellegrino, L.; Braga, D.; Grepioni, F.; Maini, L. *Chem.—Eur. J.* **2010**, *16*, 4347. (c) Brittain, H. G.; Morris, K.; Bugay, D.; Thakur, A.; Serajuddin, A. J. *Pharm. Biomed. Anal.* **1993**, *11*, 1063. (d) Sen, S.; Yu, P.; Risbud, S.; Dick, R.; Deamer, D. J. *Phys. Chem. B* **2006**, *110*, 18058. (e) Strohmeier, M.; Stueber, D.; Grant, D. M. *J. Phys. Chem. A* **2003**, *107*, 7629. (f) Schmidt, H. L.; Sperling, L. J.; Gao, Y. G.; Wylie, B. J.; Boettcher, J. M.; Wilson, S. R.; Rienstra, C. M. *J. Phys. Chem. B* **2007**, *111*, 14362. (g) Geppi, D.; Mollica, G.; Borsacchi, S.; Veracini, C. *Appl. Spectr. Rev.* **2008**, *43*, 202.
- (22) (a) Minkov, V. S.; Chesalov, Y. A.; Boldyreva, E. V. *J. Struct. Chem.* **2008**, *49*, 1061. (b) Ebert, A. A., Jr.; Gottlieb, H. B. *J. Am. Chem. Soc.* **1952**, *74*, 2806. (c) Colthup, N.; Daly, L. H.; Wiberley, S. E. *Introduction to Infrared and Raman Spectroscopy*, 3rd ed.; Academic Press: Boston, 1990.
- (23) (a) Wu, H.; Reeves-McLaren, N.; Jones, S.; Ristic, R. I. *Cryst. Growth Des.* **2010**, *10*, 988. (b) Vipagunta, S.; Brittain, H.; Grant, D. *Adv. Drug. Delivery Rev.* **2001**, *48*, 3. (c) Boldyreva, E.; Drebuschak, V.; Paukov, I.; Kovalevskaya, Y.; Drebuschak, T. *J. Therm. Anal. Calorim.* **2004**, *77*, 607. (d) Kolesov, B.; Minkov, V.; Boldyreva, E.; Drebuschak, T. *J. Phys. Chem. B* **2008**, *112*, 12827. (e) Zeitler, J.; Newnham, D.; Taday, P.; Threlfall, T.; Lancaster, R.; Berg, R.; Strachan, C.; Pepper, M.; Gordon, K.; Rades, T. *J. Pharm. Sci.* **2006**, *95*, 2486. (f) Pranzo, M.; Cruickshank, D.; Coruzzi, M.; Caira, M.; Bettini, R. *J. Pharm., Sci.* **2010**, *99*, 3731.
- (24) (a) Yang, X.; Wang, X.; Ching, C. J. *Chem. Eng. Data* **2008**, *53*, 1133. (b) Lyn, L.; Sze, H.; Rajendran, A.; Adinarayana, G.; Dua, K.; Garg, S. *Acta Pharm.* **2011**, *61*, 391. (c) Cantera, R.; Leza, M.; Bachiller, C. J. *Pharm. Sci.* **2002**, *91*, 2240. (d) Aitipamula, S.; Nangia, A. *Polymorphism: Fundamentals and Applications. In Supramolecular Chemistry: From Molecules to Nanomaterials*; Steed, J. W., Gale, P. A., Eds.; John-Wiley: New York, 2012; pp 2957–2974. (e) Zhang, J.; Tan, X.; Gao, J.; Fan, W.; Gao, Y.; Qian, S. *J. Pharm. Pharmacol.* **2013**, *65*, 44. (f) Caira, M. R.; Bourne, S. A.; Samsodien, H.; Engel, E.; Liebenberg, W.; Stieger, N.; Aucamp, M. *CrystEngComm* **2012**, *14*, 2541. (g) Blagden, N.; de Matas, M.; Gavan, P.; York, P. *Adv. Drug Delivery Rev.* **2007**, *59*, 617. (h) Qiu, Y.; Chen, Y.; Liu, L.; Zhang, G. G. *Z. Developing Solid Oral Dosage Forms: Pharmaceutical Theory and Practice*, 1st ed.; Academic Press: New York, 2009; p 75. (i) Hildebrand, J. H. *Solubility*; The Chemical Catalog Company: New York, 1924; p 206.
- (25) (a) Newman, A. *Org. Process Res. Dev.* **2013**, *17*, 457. (b) An, J.; Kim, W. *Cryst. Growth Des.* **2013**, *13*, 31. (c) An, J.; Kim, J.; Chang, S.; Kim, W. *Cryst. Growth Des.* **2010**, *10*, 3044.

(26) (a) McKellar, S. C.; Urquhart, A. J.; Lamprou, D. A.; Florence, A. J. *ACS Comb. Sci.* **2012**, *14*, 155. (b) Lopez-Mejias, V.; Knight, J. L.; Brooks, C. L.; Matzger, A. J. *Langmuir* **2011**, *27*, 7575. (c) Diao, Y.; Whaley, K. E.; Helgeson, M. E.; Woldeyes, M. A.; Doyle, P. S.; Myerson, A. S.; Hatton, T. A.; Trout, B. L. *J. Am. Chem. Soc.* **2012**, *134*, 673. (d) Roy, S.; Matzger, A. J. *Angew. Chem., Int. Ed.* **2009**, *48*, 8505.

(27) (a) Zencirci, N.; Gelbrich, T.; Kahlenberg, V.; Griesser, U. J. *Cryst. Growth Des.* **2009**, *9*, 3444. (b) Kendrick, J.; Montis, R.; Hursthouse, M. B.; Leusen, F. J. J. *Cryst. Growth Des.* **2013**, *13*, 2906. (c) Cornel, J.; Lindenberg, C.; Mazzotti, M. *Cryst. Growth Des.* **2009**, *9*, 243.

(28) Kraus, N.; Nolze, G. *Powder Cell, A Program for Structure Visualization, Powder Pattern Calculation and Profile Fitting*, version 2.3; Federal Institute for Materials Research and Testing: Berlin, Germany, 2000.